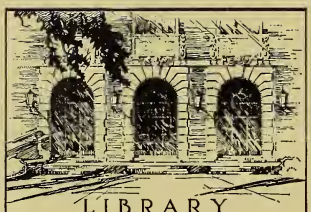

Westinghouse Electric Corporation
Air Arms Division
Attn: Librarian (Antenna Lab)
P. O. Box 746

Wheeler Laboratories
Attn: Librarian (Antenna Lab)
Box 561
Smithtown, New York

Electrical Engineering Research
Laboratory
University of Texas
Box 8026, Univ. Station
Austin, Texas

University of Michigan Research
Institute
Electronic Defense Group
Attn: Dr. J. A. M. Lyons
Ann Arbor, Michigan

New Mexico State University
Head Antenna Department
Physical Science Laboratory
University Park, New Mexico

Bell Telephone Laboratories, Inc.
Whippany Laboratory
Whippany, New Jersey
Attn: Technical Reports Librarian
Room 2A-165

Robert C. Hansen
Aerospace Corporation
Box 95085
Los Angeles 45, California

Dr. D. E. Royal
Ramo-Wooldridge, a division of
Thompson Ramo Wooldridge Inc.
8433 Fallbrook Avenue
Canoga Park, California

Dr. S. Dasgupta
Government Engineering College
Jabalpur, M.P.
India

Dr. Richard C. Becker
10829 Berkshire
Westchester, Illinois

Dr. Harry Letaw, Jr.
Raytheon Company
Surface Radar and Navigation
Operations
State Road West
Wayland, Massachusetts

Dr. Frank Fu Fang
IBM Research Laboratory
Poughkeepsie, New York

Mr. Dwight Isbell
1422 11th West
Seattle 99, Washington

Dr. A. K. Chatterjee
Vice Principal
Birla Engineering College
Pilani, Rajasthan
India

Antenna Laboratory

Technical Report No. 55

AN INVESTIGATION OF THE NEAR FIELDS ON THE CONICAL EQUIANGULAR SPIRAL ANTENNA

by

O. L. McClelland

Contract AF33(657)-8460

Project No. 6278, Task No. 40572

May 1962

Sponsored by:

AERONAUTICAL SYSTEMS DIVISION

Electrical Engineering Research Laboratory
Engineering Experiment Station
University of Illinois
Urbana, Illinois

ACKNOWLEDGEMENT

The author wishes to thank all the members of the Antenna Laboratory Staff for their assistance and encouragement. He is particularly indebted to his advisor, Dr. John D. Dyson, whose interest and supervision have made this report possible. Appreciation is extended to Dr. R. Mittra for the many helpful discussions and for his continued interest in the investigation.

ABSTRACT

The current distribution has been measured on a conical equiangular spiral antenna. A correlation between the operation of the conical log-spiral antenna and the operation of the uniform circular bifilar helix is established by utilizing a general theory of backward wave radiation from periodic structures. Operation beyond the normal frequency limits has been explored and discussed. The arms of the antenna were constant diameter conductors. The effects of this deviation from the ideal design, which calls for a linearly increasing diameter, have been observed. The far field measurements, giving for example the center of phase location, agrees with the near field probing.

CONTENTS

ILLUSTRATIONS

ILLUSTRATIONS (Continued)

1. INTRODUCTION

The introduction in 1954 of the concept of frequency independent antennas led to an important breakthrough in the antenna field[1]. Many versions of these antennas have been studied since that time. Of these, possibly the two most practical versions from simplicity of construction are the log-periodic dipole array[2,3] and the wire-arm version of the conical log-spiral[4].

In an effort to provide information that would lead to a better understanding of the operation of the conical log-spiral antenna, an experimental investigation was made of the amplitude and phase of the near fields on one antenna. The purpose of this paper is to present this data and to indicate how it correlates with a general theory of backward wave radiation from periodic structures[5].

2. THE BASIC ANTENNA

The conical log-spiral antenna with its associated coordinate system is shown in Figure 1. Only the center line of the antenna arm has been shown because the antenna dealt with here was the constant width arm version of the conical log-spiral antenna. If one looks at the triangle formed by $ad\varphi$, $d\rho$ and ds where a is the radius of the cone at the element of circumference $ad\varphi$, $d\rho$ is an element of the radius vector, and ds is an element of arm length, it will be seen that

$$\tan \alpha = \frac{ad\varphi}{d\rho}$$

but

$$\alpha = \rho \sin \theta_o$$

where θ_o is the half angle of the cone and therefore

$$\frac{d\rho}{\rho} = \frac{\sin \theta_o}{\tan \alpha} d\varphi$$

giving the equation for the equiangular curve

$$\rho = \rho_o \exp\left(\frac{\sin \theta_o}{\tan \alpha} \varphi\right)$$

where ρ_o is a constant factor arising from the tip truncation.

Again looking at the same triangle, it is observed that

$$d\rho = \cos \alpha \, dS$$

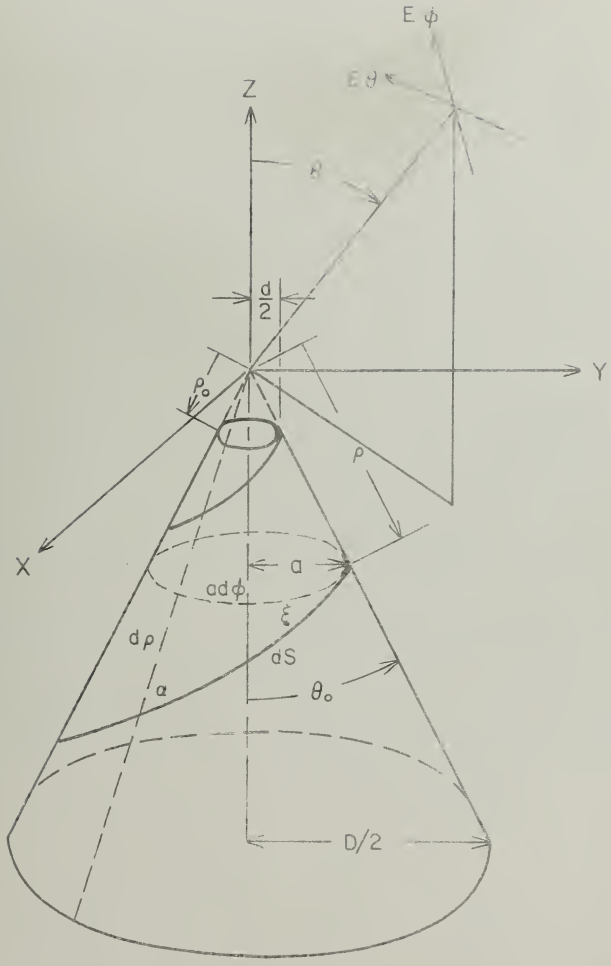

Figure 1. A conical log-spiral antenna with its associated coordinate system

or

$$\rho = S \cos \alpha + \text{constant} \quad .$$

In the case where there is no truncation, i.e., when $S = 0$ for $\rho = 0$, the constant is zero yielding

$$\rho = S \cos \alpha$$

If the cone has been truncated, $S = 0$ but $\rho = \rho_o$. Then the constant $= \rho_o$ and

$$\rho = S \cos \alpha + \rho_o$$

It will be convenient later to speak in terms of pitch angle as commonly defined for the cylindrical helix. The pitch angle ξ is the complement of the constant spiral angle α which the curve makes with a radius vector of the cone. To summarize the results and add a few obvious relationships, we have

In terms of spiral angle α	In terms of pitch angle ξ
$\rho = \rho_o \exp \left[\frac{\sin \theta_o}{\tan \alpha} \varphi \right]$	$\rho = \rho_o \exp [(\sin \theta_o \tan \xi)\varphi]$
$\rho = S \cos \alpha$	$\rho = S \sin \xi$

and for both cases

$a = \rho \sin \theta_o$	$D = \rho_{max} \sin \theta_o$
$d = 2 \rho_o \sin \theta_o$	$C = 2\pi a$

3. BACKWARD WAVE RADIATION FROM THE CONICAL LOG-SPIRAL

In the spring of 1961 Mayes, Deschamps, and Patton[5] indicated that frequency independent antennas could be analyzed by considering them to be locally periodic structures whose period varies slowly, increasing with distance from the apex. At any given frequency there is a region on the spiral where the current is phased properly to produce radiation toward the apex and hence produce backward wave radiation. It was postulated that this region on the conical log-spiral antenna could be approximated by a bifilar helix with parameters equal to the average conical spiral parameters over this region.

In an effort to apply this idea to the conical antenna, it is instructive to consider some of the techniques which have been useful in the analysis of helices. The Brillouin diagram, relating the propagation constant h on the surface of the helix to the frequency ω or to $k = \omega/c$ the propagation constant in free space, has been a convenient tool in the analysis of periodic structures and in particular the helix[6].

In the derivation of the Brillouin or k-β for the helix, it has been shown[7,8] that h is real in the regions defined by the boundaries

$$m + \frac{ka}{\cot \xi} < \frac{|h|a}{\cot \xi} < m - \frac{ka}{\cot \xi} \quad ;$$

m is a positive real integer. A consequence of this is that for h to be real $ka/\cot \xi \leq 1$ for the bifilar helix. The unshaded areas in Figure 2 designate the regions where h is real. Sensiper[7] has shown that the solutions of the determinantal equation can be approximated by the line $ka/\cot \xi = ha/\cot \xi \sin \xi$, which can be interpreted as a wave progressing at the speed of light

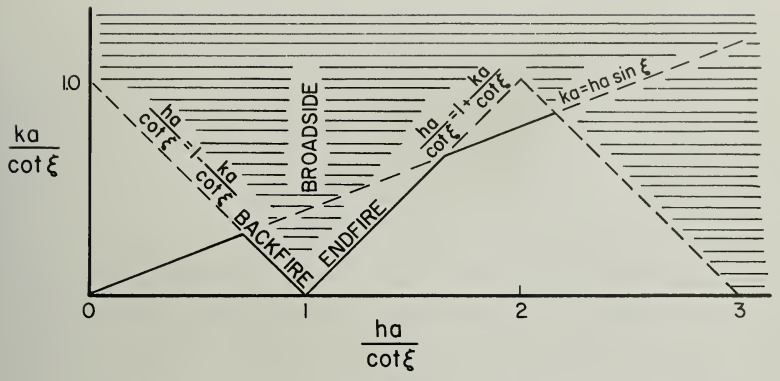

Figure 2a. Typical k-β diagram for bifilar helix when considering operation along the cylinder surface

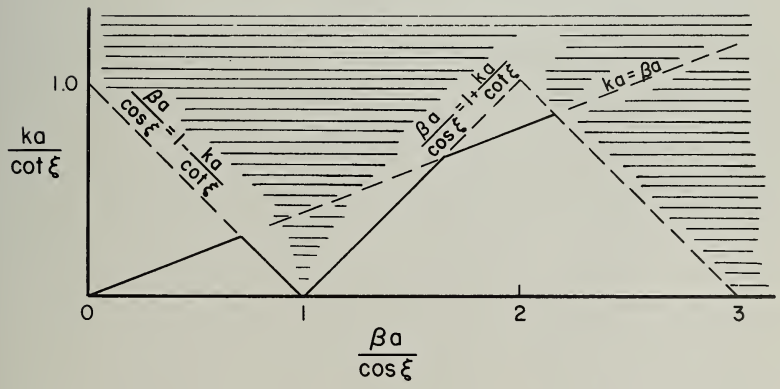

Figure 2b. Typical k-β diagram for bifilar helix when considering operation along the conductor

along the thin tape, and the m=1 boundaries of the regions discussed above as are shown in Figure 2a. As Sensiper has indicated, for many practical purposes, these roots are the only ones which may need to be considered on the cylinder surface. It was felt, since the data were taken along the conductor, that a k-β diagram as shown in Figure 2b was more applicable for this presentation. This diagram is essentially the same as Figure 2a, where $\beta = h \sin \xi$, the propagation constant along the conductor is used as the variable. It should be noted here that the relation shown in this diagram should be applicable only to an infinite, thin-tape helix. When the tape is not thin, the current progression will deviate from the speed of light. It has been demonstrated, however, that experimental data taken on a finite helix agrees quite well with the diagram[7].

The locus of the propagation constant in Figure 2b will give a value of βa real for each value of ka. In the case of the helix, the radius a and pitch angle ξ are constants. As the frequency is increased, the value of β scans as the diagram predicts. In the case of the log-spiral, the pitch angle ξ is constant, but the radius a increases linearly with distance from the tip. Since β is a function of a at any particular frequency, β changes with distance from the apex.

4. PHYSICAL CONSTRUCTION CONSIDERATIONS

Two antennas were constructed, one model to operate from approximately 150 mc to 700 mc, and a smaller model with the same tip diameter and construction but with a base diameter just one-half the size of the large model. Therefore, the smaller model had a frequency range from approximately 300 mc to 700 mc. This particular frequency range was chosen to insure that the probing system used during the near field measurements would be small with respect to the wavelength. Most of the data were taken on the small model. Near field measurements were made on the large model in order to observe the effects of the base truncation and to observe a lower frequency of operation. The spiral angle α and one-half the enclosed cone angle θ_o were selected to insure a small back lobe on the antenna[4]. One-half inch copper tubing was chosen as the constant width arm for ease of construction and probe mounting. The physical dimensions of these antennas are given in Figure 3.

The two copper arms were fed by the infinite balun method, i.e., by inserting a coaxial cable inside one arm with its outer conductor bound to the "feed arm" and its center conductor connected to the "dummy arm" as shown in Figure 5. This gives an anti-symmetric, slit-generator feed which should be as frequency independent as the antenna itself. The bullet-shaped end on the dummy arm was selected for optimum impedance characteristics.

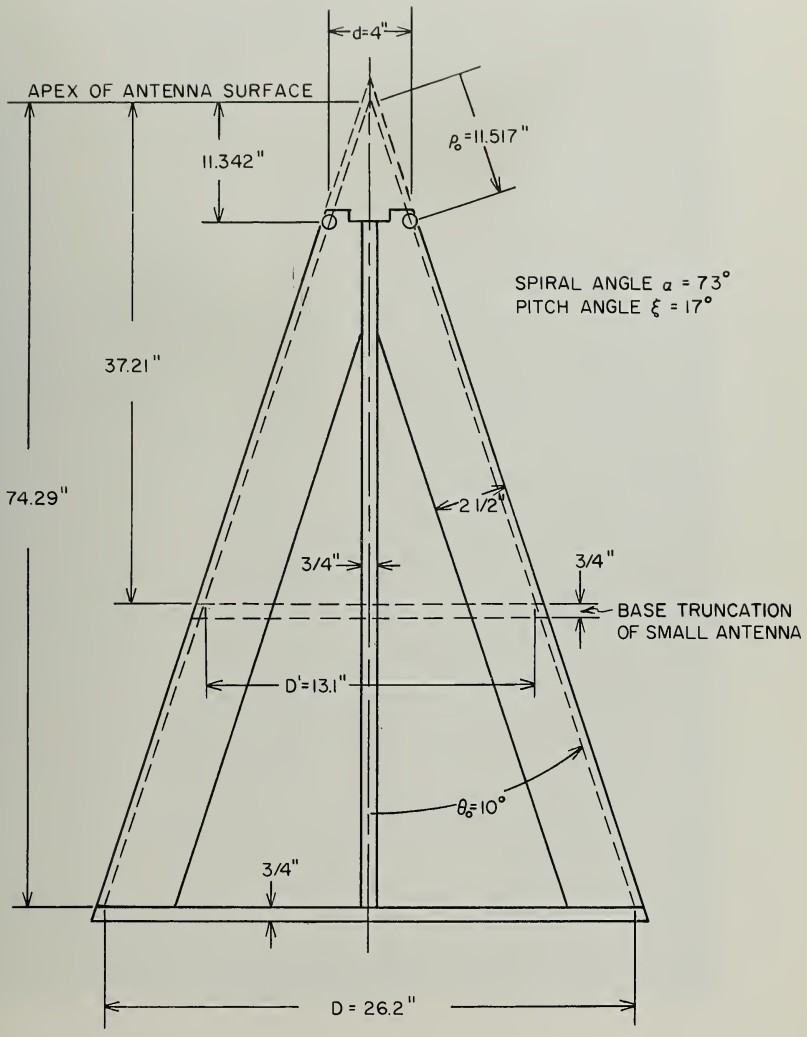

Figure 3. Physical dimensions of the test antennas

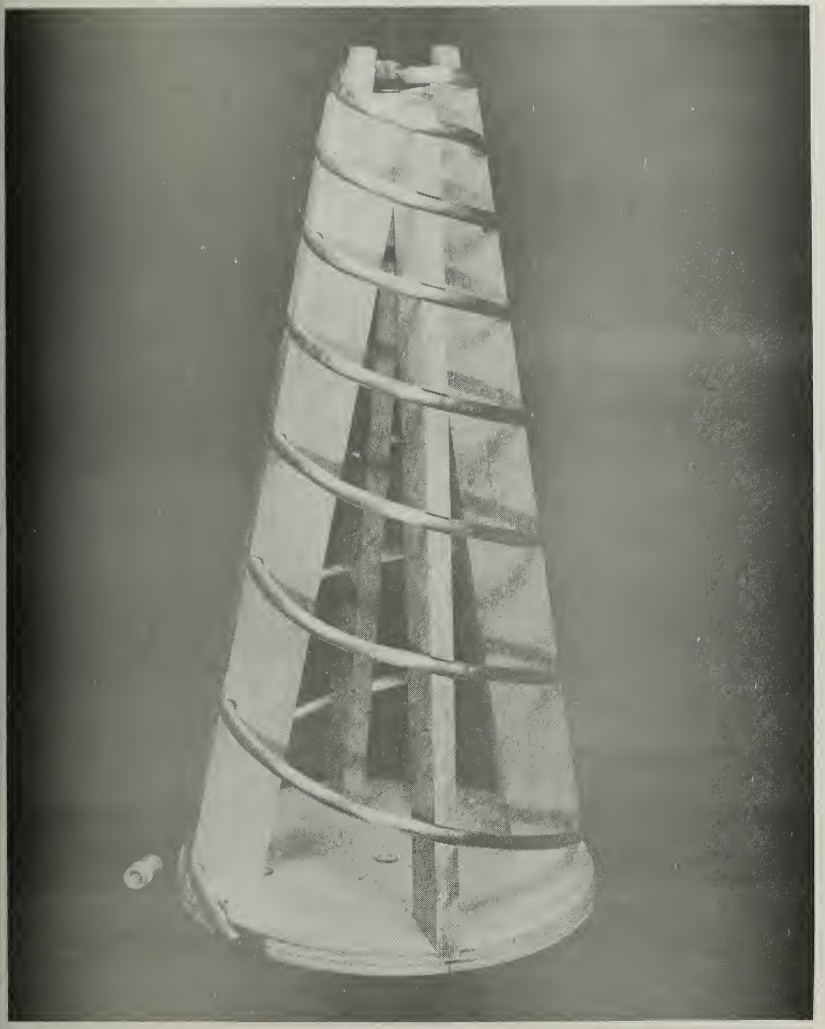

Figure 4. Photograph of the small test antenna

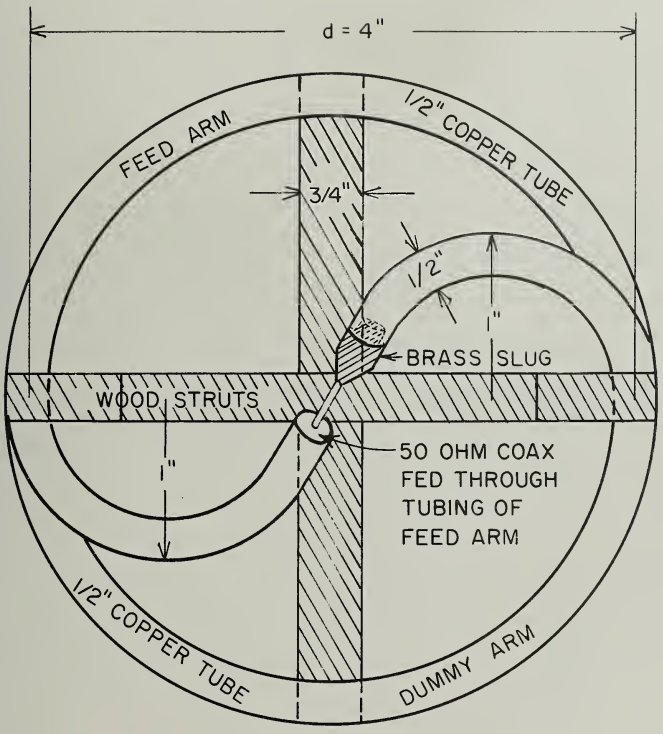

Figure 5. The feed region of the test antenna

5. MEASUREMENT CONSIDERATIONS

Throughout the entire experimental program no attempt was made to prove that the wire version of the conical log-spiral antenna was a "frequency independent" antenna since Dyson[4] has already established this fact. A definition of frequency independence is given by R. L. Carrel. "By frequency independence as applied to an antenna, it is meant that the observable characteristics of the antenna such as the field pattern and input impedance vary negligibly over a band of frequencies within the design limits of the antenna, and that this band may be made arbitrarily wide merely by properly extending the geometry of the antenna structure. The ultimate band limits of a given design are determined by non-electrical restrictions: size governs the low frequency limit, and precision of construction governs the high frequency limit."[3] The antenna was designed to have essentially constant impedance and patterns over a two to one band. Measurements were made over a four to one band in order to investigate the operation beyond the normal limits.

The near field measurements consisted of measuring the relative amplitude and relative phase of the current flowing along the conductor of the antenna. A signal proportional to this current was received from a small shielded current loop probe[9] shown in Figure 6. The loop probe was placed on the end of a sufficiently long piece of .050 inch microdot cable which was allowed to follow the surface of the antenna arm. The loop itself was mounted on a beryllium copper clip which provided a means of fastening the probe to the one-half inch copper tube arms of the antenna. Calibrated positions were inscribed on the arms to facilitate accurate positioning of the probe.

It was necessary to determine if the presence of the microdot cable was

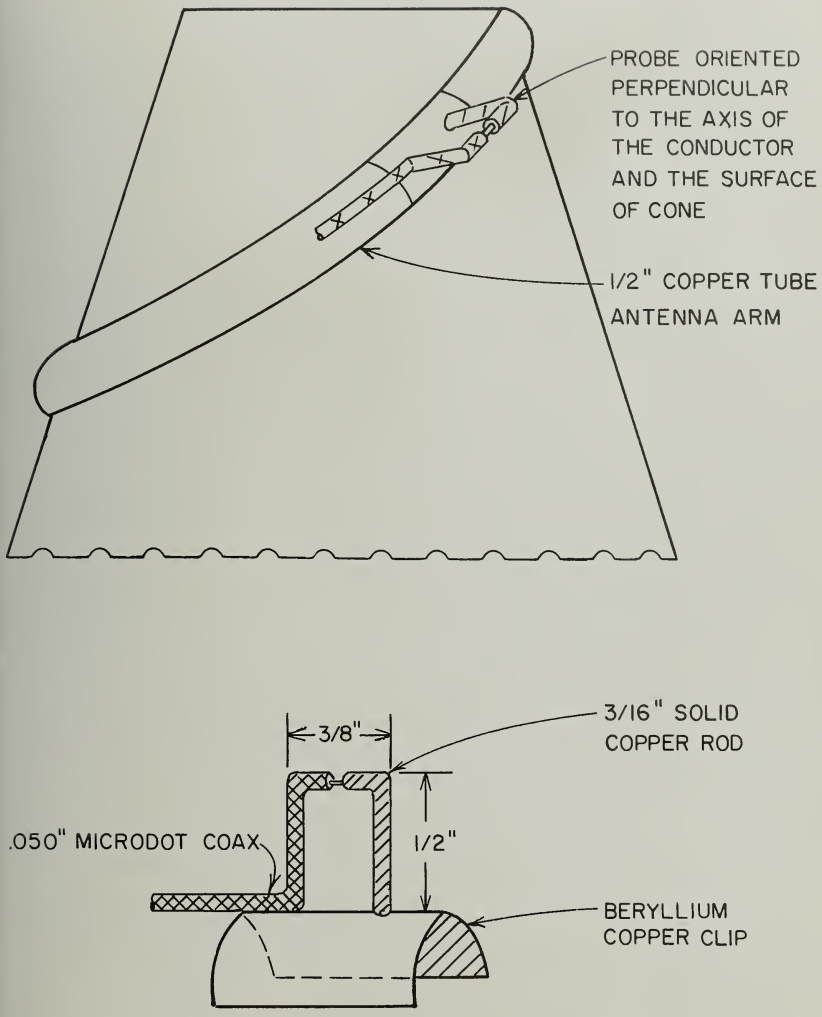

Figure 6. Detail of the probe used for the near field measurements

disturbing the near fields on the antenna arms. Only negligible deviations in the signal level could be determined when a piece of microdot cable was placed in various locations on the arm around the loop. Also, no deviation occurred when an additional shield was placed around the microdot cable indicating negligible leakage from the cable. All data was recorded relative to the same initial position on the antenna arm. No attempt was made to approach the slit-generator feed beyond the point where the antenna arm left the true equiangular curve. Data were taken at approximately 0.1λ intervals along the arm progressing down the antenna. To minimize flexing, the microdot cable was allowed to droop down in a large loop.

5.1 Relative Amplitude Measurements

A block diagram of the circuit used for the amplitude measurements is shown in Figure 7. The output of the RF power oscillator, delivering a continuous wave, was padded and filtered before delivery to the antenna. Two signal taps were provided to allow both frequency and amplitude monitoring. The stubs were tuned to a maximum probe signal level when the probe was placed in the reference position discussed previously. The addition of the 100 mc low pass filter was found to be necessary since the filter provided in the crystal mixer was not adequate to block the RF signal from passing through the mixer to the 30 mc IF amplifier. It was found that a power output of several watts was needed in order to achieve an adequate dynamic range.

5.2 Relative Phase Measurements

The relative phase measuring circuit is diagrammed in Figure 8. The input system to the antenna was similar to the system used for magnitude measurements except the power was not monitored. If the power had drifted, both the reference signal level and the probe signal level would have drifted together and would

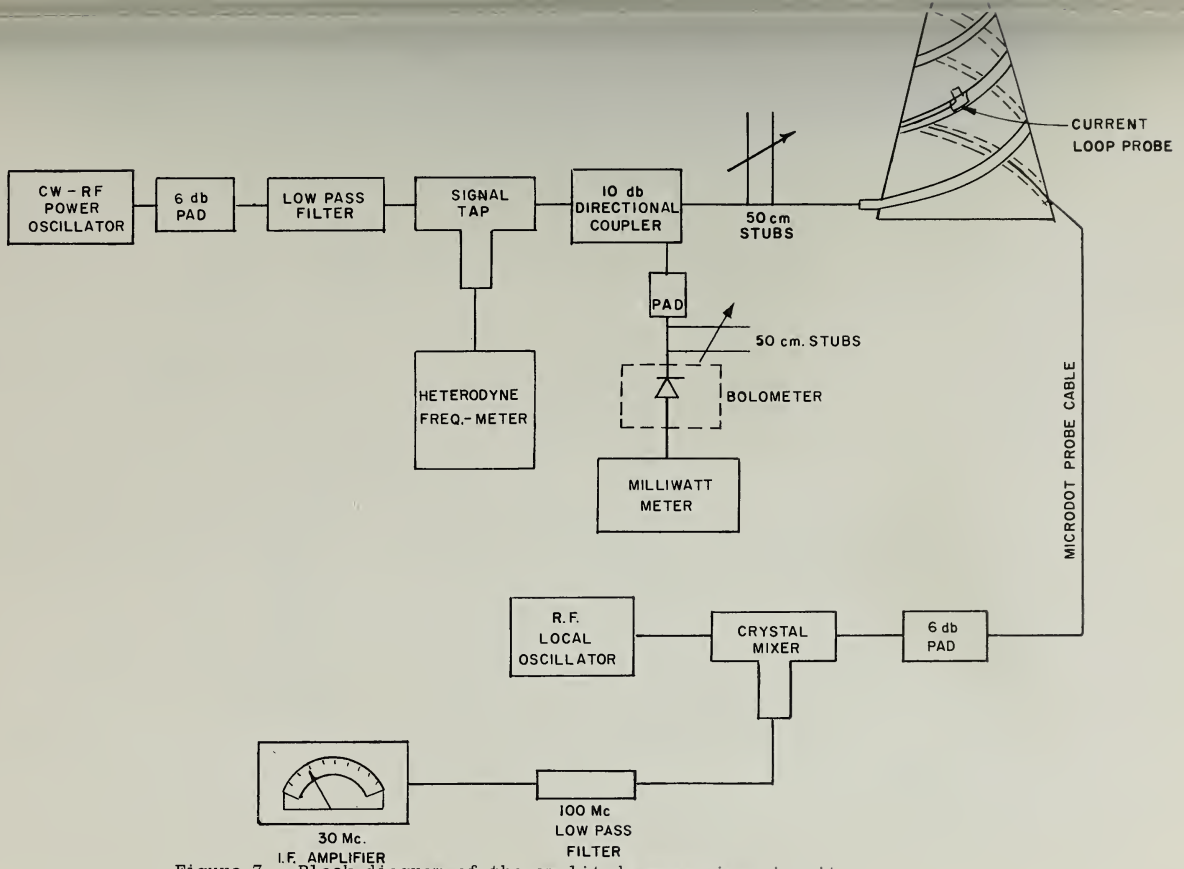

Figure 7. Block diagram of the amplitude measuring circuit

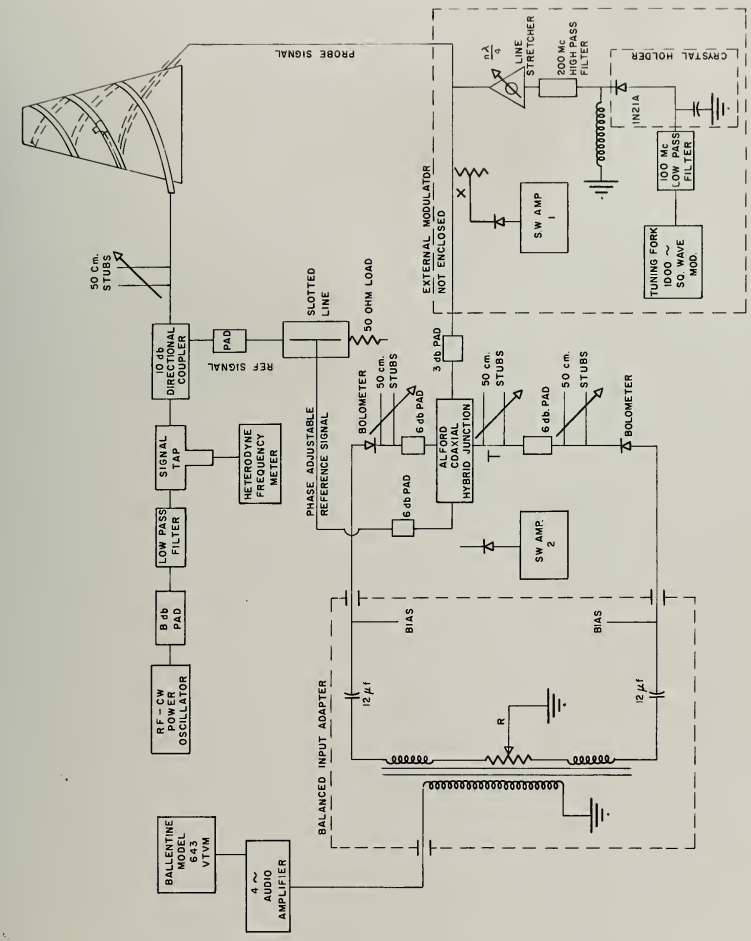

Figure 8. Block diagram of the phase measuring circuit

not have disturbed the measurement.

The theory of the measurement was as follows. The probe signal was externally modulated and fed into either the series or shunt arm of the coaxial hybrid junction. Likewise, the CW reference signal, the phase of which could be adjusted by means of a matched slotted line, was inserted into the remaining shunt or series arm of the hybrid. The outputs of the hybrid, one of the RF phasor sum and the other the RF phasor difference, were independently matched and detected. The two detected audio signals, one the magnitude of the sum, and the other the magnitude of the difference, were subtracted in the balanced input adapter. The difference of these two magnitudes was applied to the audio amplifier and read out on the Ballentine VTVM

As can be seen by the phasor relationships in Figure 9, a sharp null should be observed when the two input signals are in phase quadrature. The phase measurement was somewhat insensitive to the difference in amplitude between the two input signals. A precise null was always present, no matter how large the difference in the amplitudes. Of course, keeping the null above noise was a problem when either the two signals were both small or the difference was great. In either case, the entire standing wave could have been engulfed in the noise. For these particular measurements it was found that the null position could be located with a reasonable degree of accuracy when the relative difference between the probe signal and the reference signal increased to 25 db.

In this measurement, only the probe signal was modulated to provide a sharper null at R. The only error due to the unmodulated reference signal was a leakage through the hybrid junction. Even though the unmodulated signal,

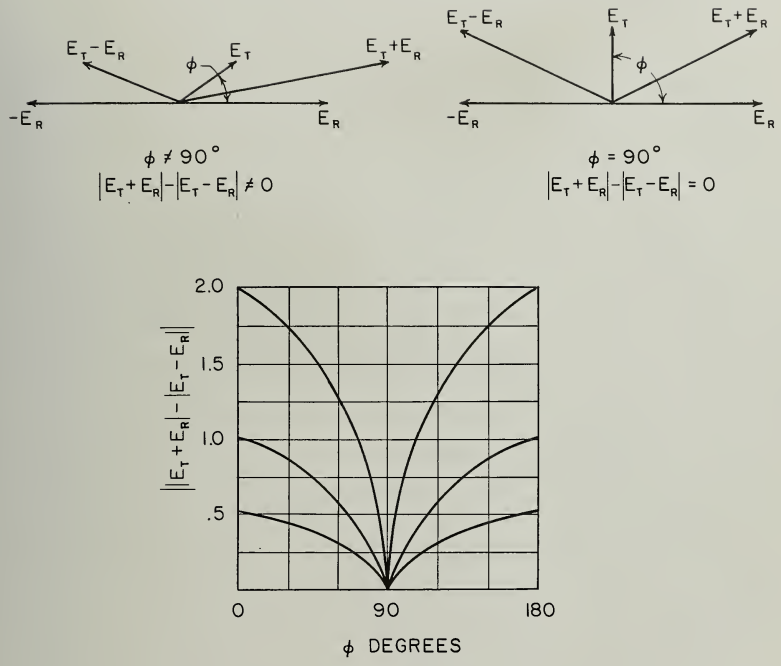

Figure 9. Balanced detection phase measuring system nulls and phasor relationships

which at times was much larger than the modulated probe signal, was present at the detectors, only a DC component was present at the transformer In a well balanced system the isolation between inputs is in the order of 60 to 70 db.

The following procedure was used to balance the hybrid junction after each change in frequency. Refer again to Figure 8. The external modulator was applied to a signal taken from the 10 db directional coupler. This modulated signal was used throughout the balance procedure. This method was used, as opposed to modulating the source, in order that the frequency used during the balancing procedure would be the same as the frequency used during the phase measurement. Modulation applied directly to the source will shift the frequency. The line stretcher in the modulator was adjusted for maximum deflection on SW amplifier No. 1. At this maximum the distance from the crystal to the probe line was some multiple of a quarter wavelength allowing an optimum switching action to be applied to the RF signal. The hybrid junction and the stubs T were removed from the circuit. Each arm, attached to the outputs of the hybrid, was balanced individually. The modulated signal was applied to one of the detection arms with the resistor R placed for maximum signal observed on the Ballentine VTVM. The stubs in the detection arms were also adjusted for a maximum on this meter. The same procedure was carried out on the other detection arm. In this particular circuit the difference in detected signal from the two arms was less than 0.5 db.

The balanced arms were connected to the hybrid junction and the stubs T. The modulated signal was then increased in amplitude and applied to one input of the hybrid through a 6 db pad. The other input was monitored with SW amplifier No. 2 through a detector and a 6 db pad. The stubs were then adjusted

for a minimum on this meter which was measuring directly any leakage through the hybrid due to unbalance on the output arms. When a minimum was observed, the stubs T were in such a position as to have balanced out any difference in impedance seen by the two output arms. The previous step only insured that the sensitivity of both detectors was the same and did not insure balanced input impedances. Next, the output, which was monitored, was then terminated in a matched load. The resistance R was adjusted for a minimum deflection on the Ballentine VTVM. These last two steps were repeated to insure the highest degree of balance. This completed the balancing procedure and the circuit in Figure 8 was then reassembled and ready for measurements.

The system was checked by two methods. The first was to measure a known phase shift and the second to observe distances between null positions. The first check was performed on the system by measuring a calibrated delay line which was inserted into the probe line. The balancing procedure was continued until the error in measuring the delay line was less than one percent. The maximum error measured after a set of data was taken was less than two percent. The increase in error was accountable to a drift in frequency during the measurement on the antenna. The second check depends upon the fact that if the hybrid junction was perfectly balanced, the distance between consecutive null points would be one-half of one free-space wavelength. Therefore, during the measurement, the distances between nulls were tabulated and compared as the phase was shifted and successive nulls were followed. If the distance between nulls began to deviate, one from another, it was an indication that the hybrid was becoming unbalanced. If the hybrid was unbalanced, the sum of the distances among three consecutive nulls was equal to a free-space wavelength; but the distance between two consecutive nulls was not one-half of one free-space wavelength.

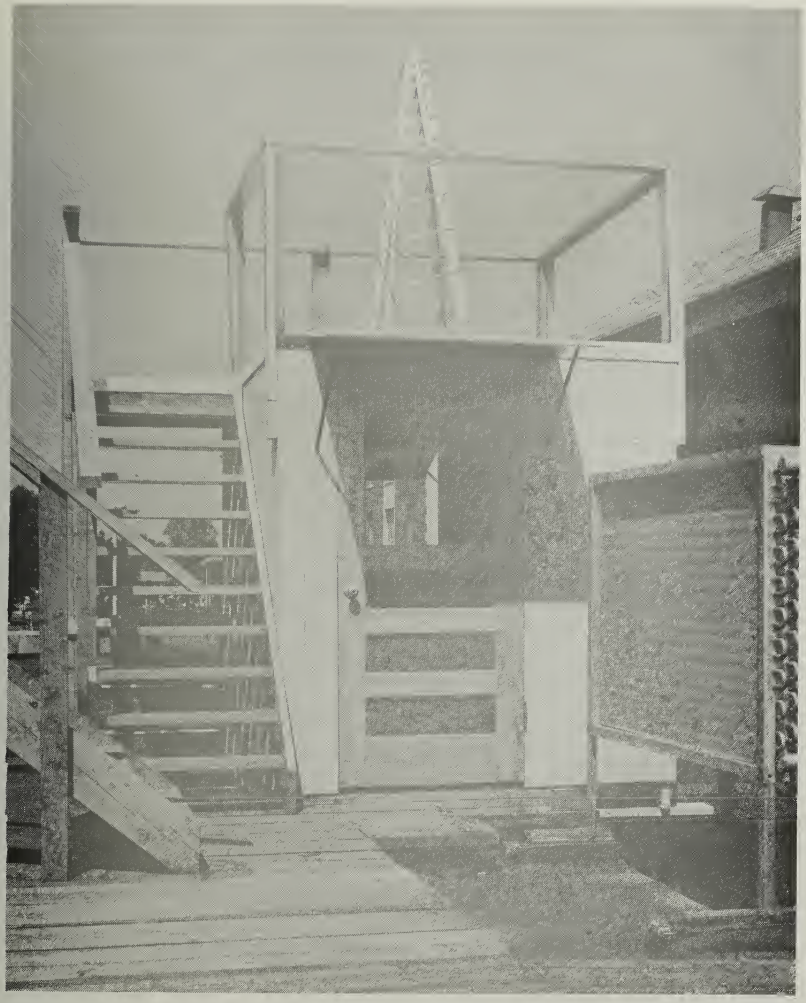

Figure 10. Photograph of the large antenna mounted in the measurement site

6. EXPERIMENTAL RESULTS

6.1 The Current Distribution

The relative magnitude of the current distribution has been measured at six frequencies, from 300 mc to 800 mc, on the small model and at four frequencies, from 200 mc to 800 mc, on the large model. The relative phase of the current was measured at five frequencies from 400 mc to 800 mc on the small model only. This data is displayed in Figures 11 through 23 inclusive.

Figures 11 through 17 indicate two items of interest:

(1) A rapid decay in the amplitude over the first portion of the structure. The rate of decay over this first portion tended to be frequency dependent, i.e., increasing rate with increasing frequency. This indicated that the rate of decay was a function of arm width in wavelengths as was noted by Dyson[10] on the planar structure.

(2) The average phase velocity along the arms in the initial region was always that of the speed of light or greater indicating a fast wave progressing along the arm from tip to base. The phase velocity also tended to be a function of arm width in wavelengths.

Figure 18 is a composite curve of the relative amplitude curves shown in Figures 11 through 17, and Figure 19 is a composite curve of the relative phase curves. These two graphs were formed by referencing the initial amplitudes and phases such that the first regions of the curves were practically coincident. It must be admitted that this was rather arbitrary, but it did give an indication of the amount of energy which was being dissipated in the quasi dipole feed previously shown in Figure 5. Radiation from the feed section will be discussed later.

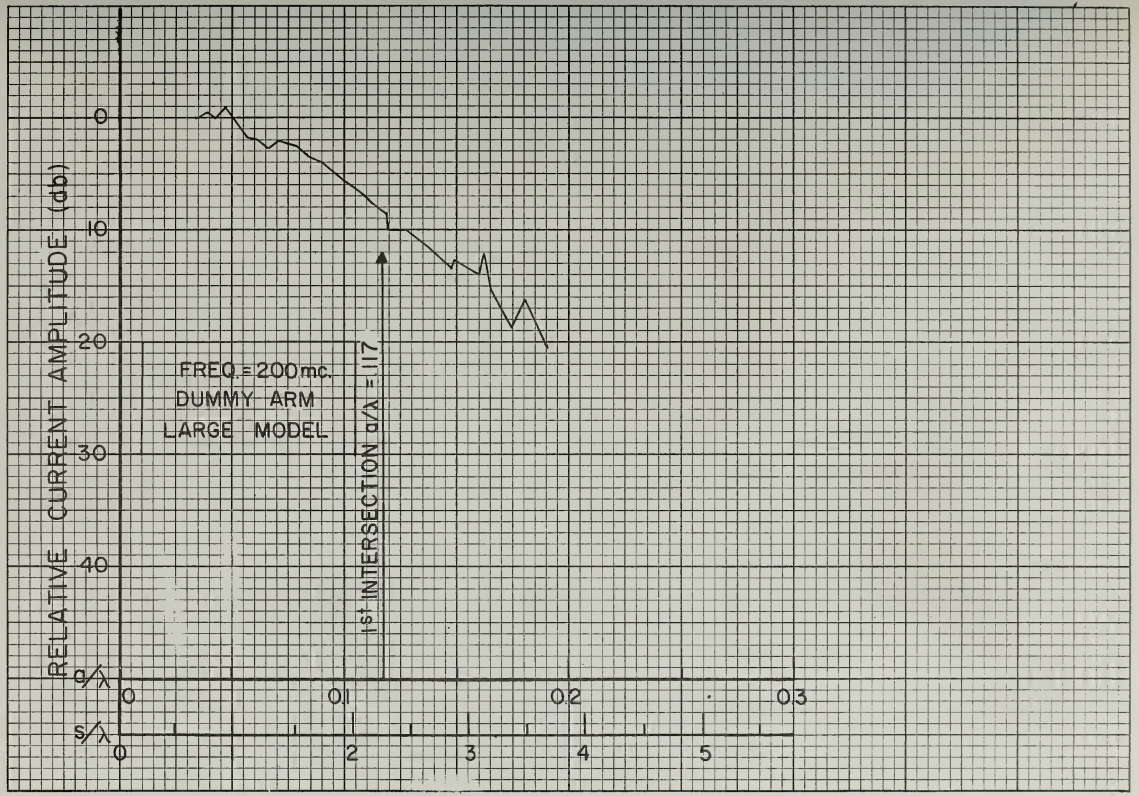

Figure 11. The current amplitude along the arm at 200 mc

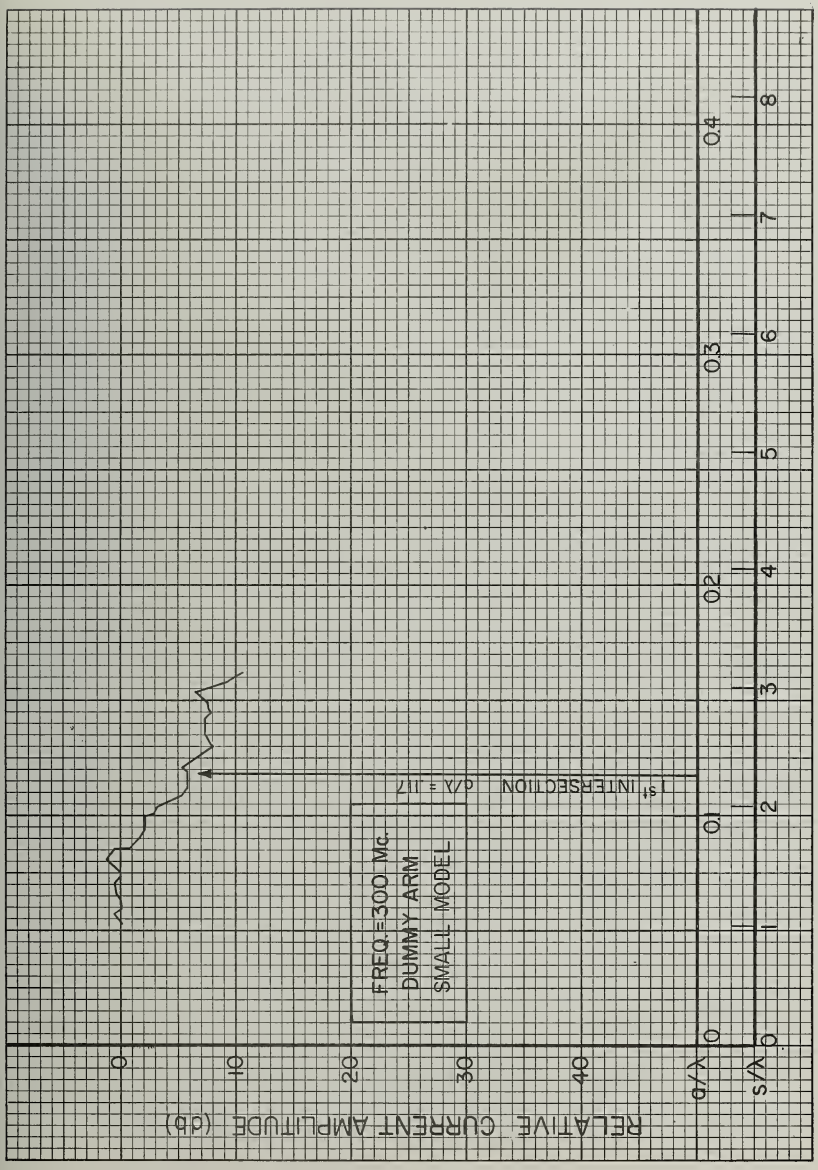

Figure 12. The current amplitude along the arm at 300 mc

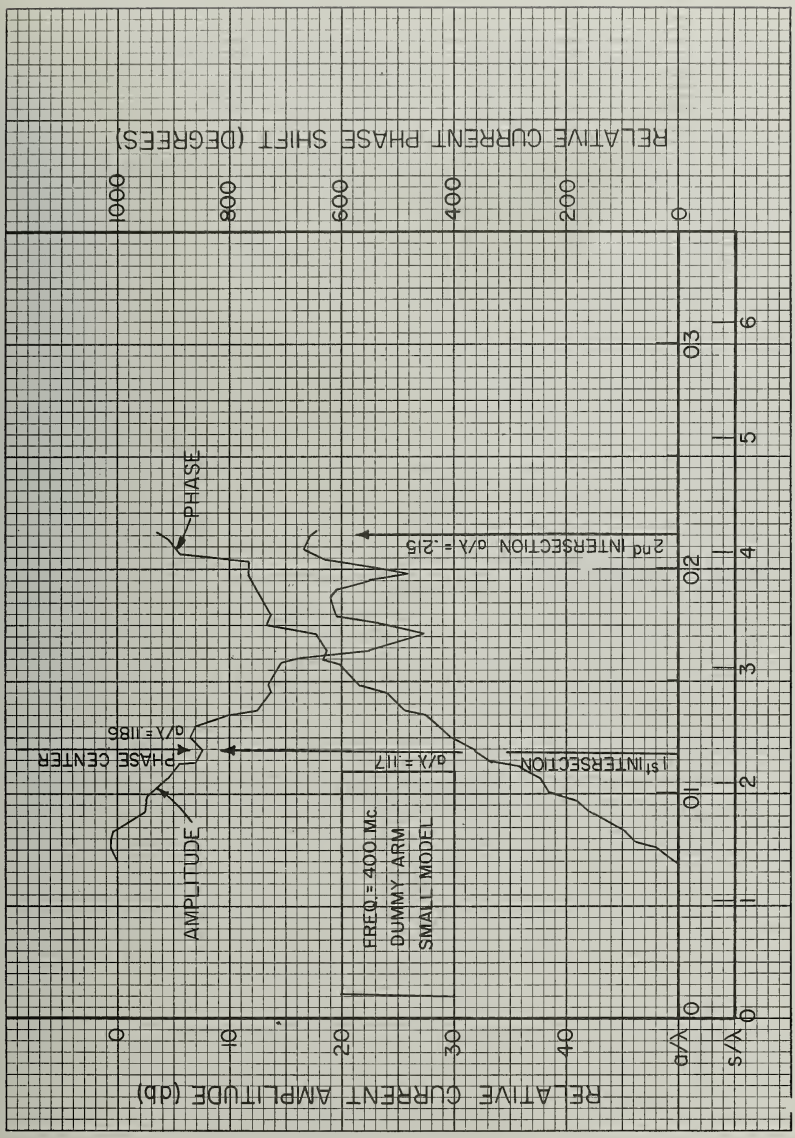

Figure 13. The current distribution along the arm at 400 mc

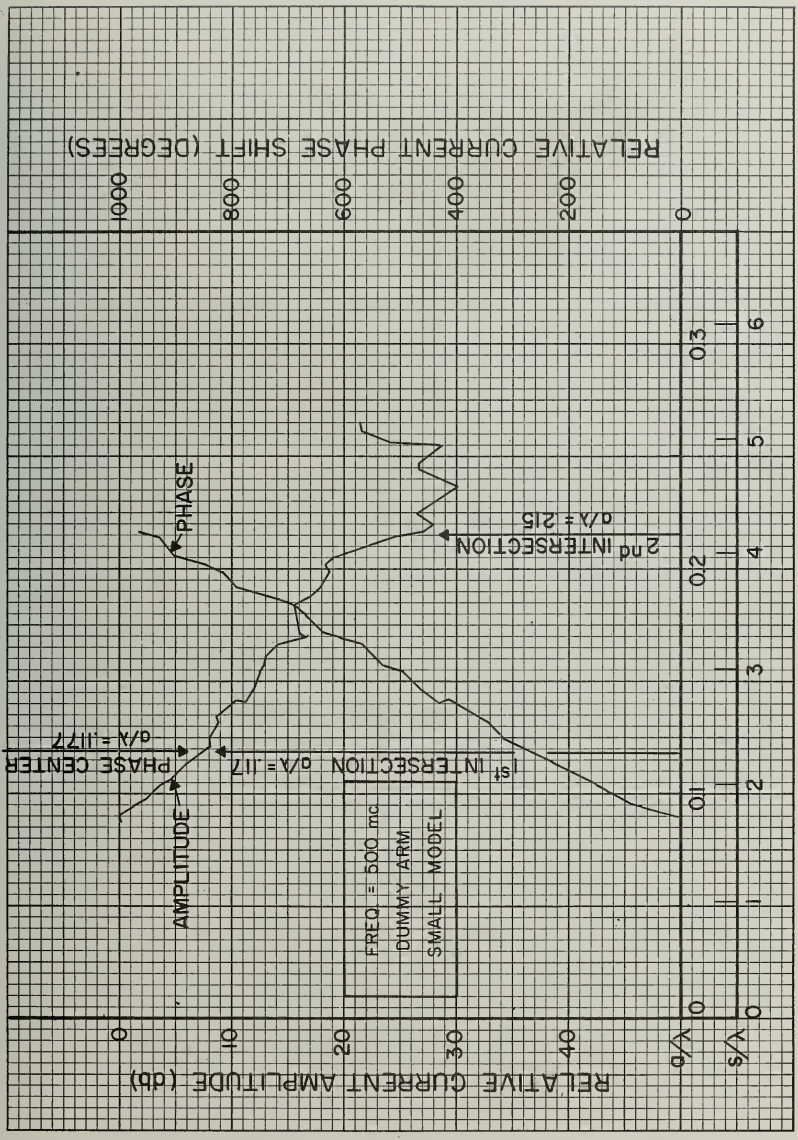

Figure 14. The current distribution along the arm at 500 mc

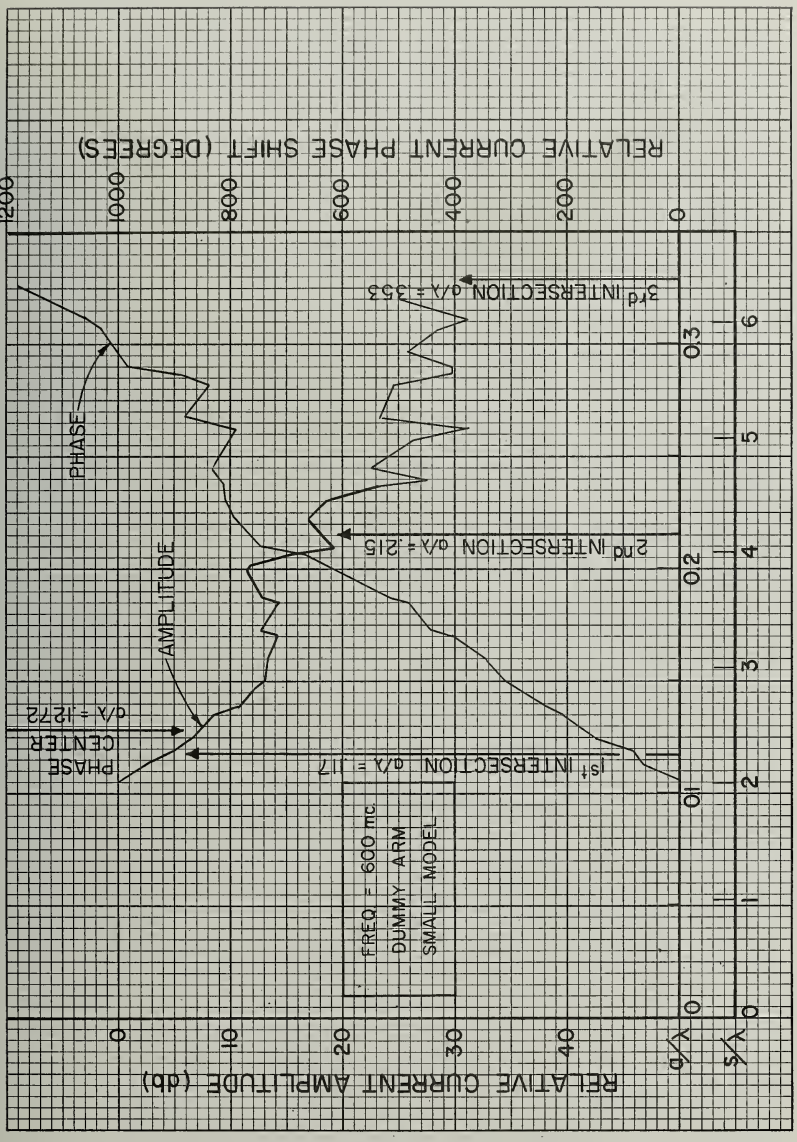

Figure 15. The current distribution along the arm at 600 mc

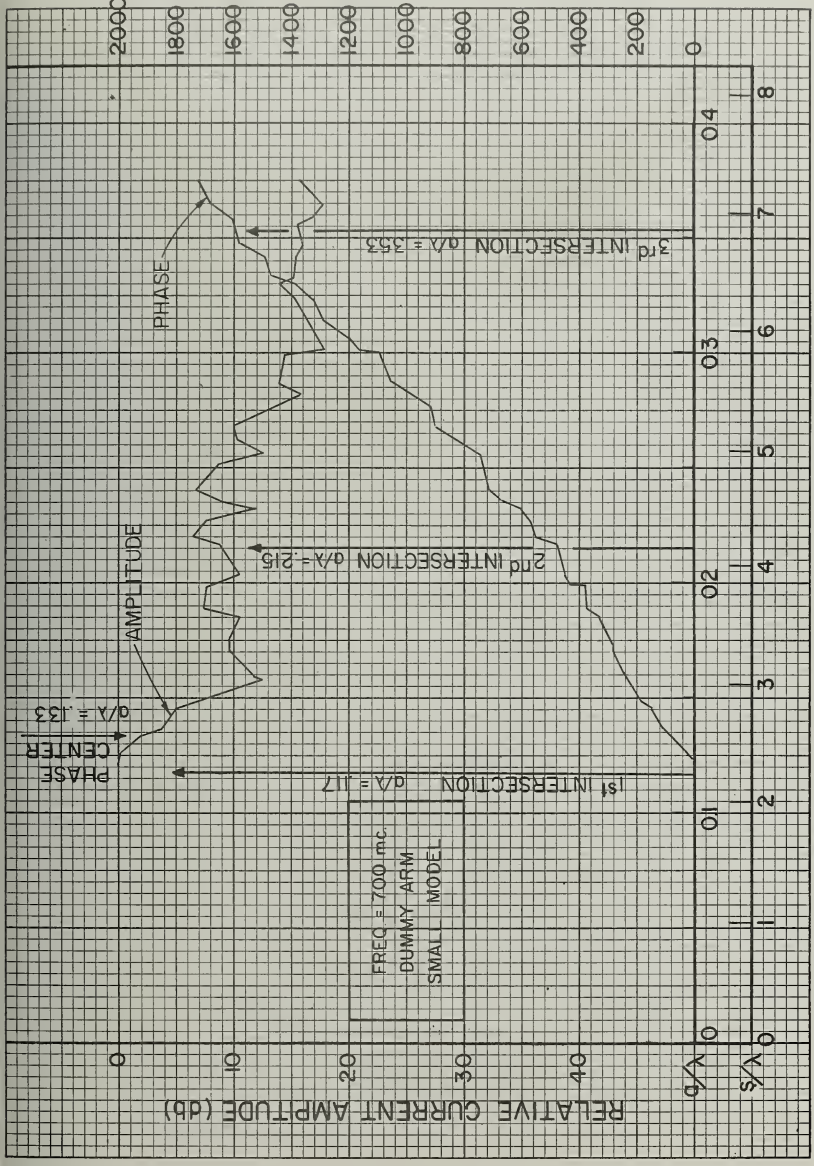

Figure 16. The current distribution along the arm at 700 mc

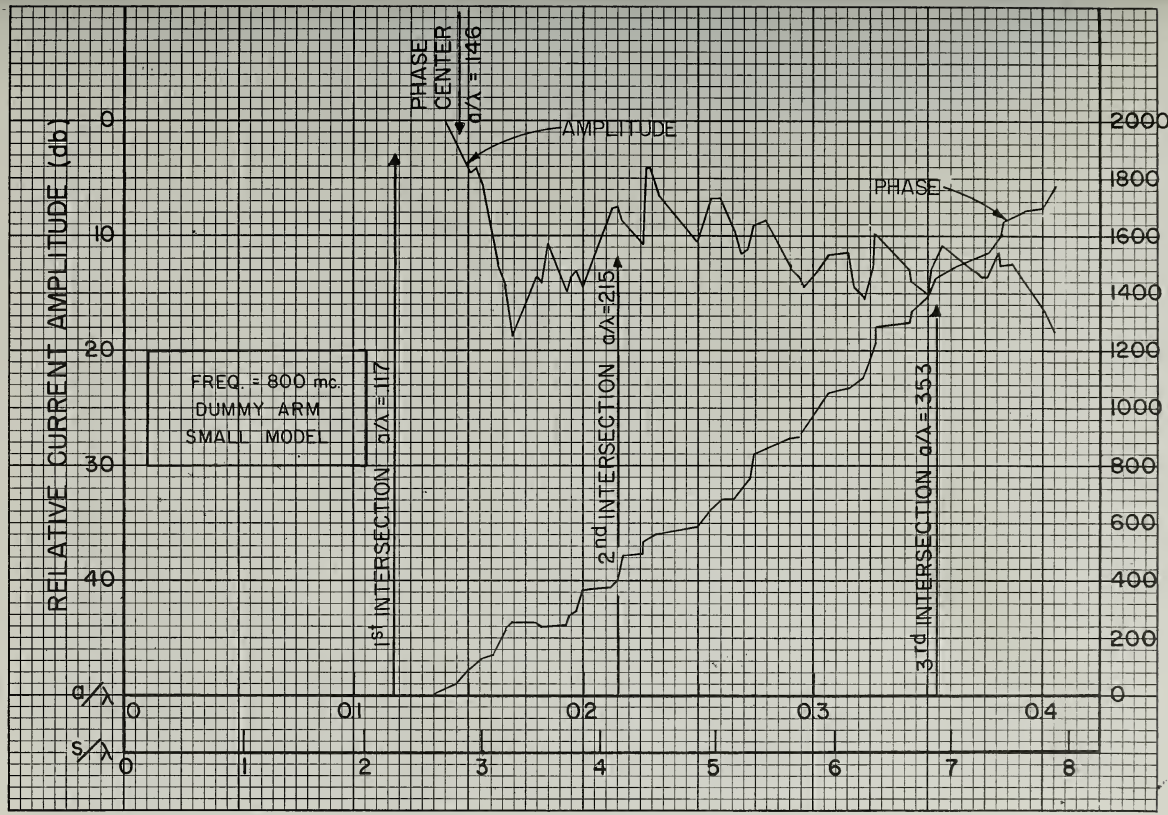

Figure 17. The current distribution along the arm at 800 mc

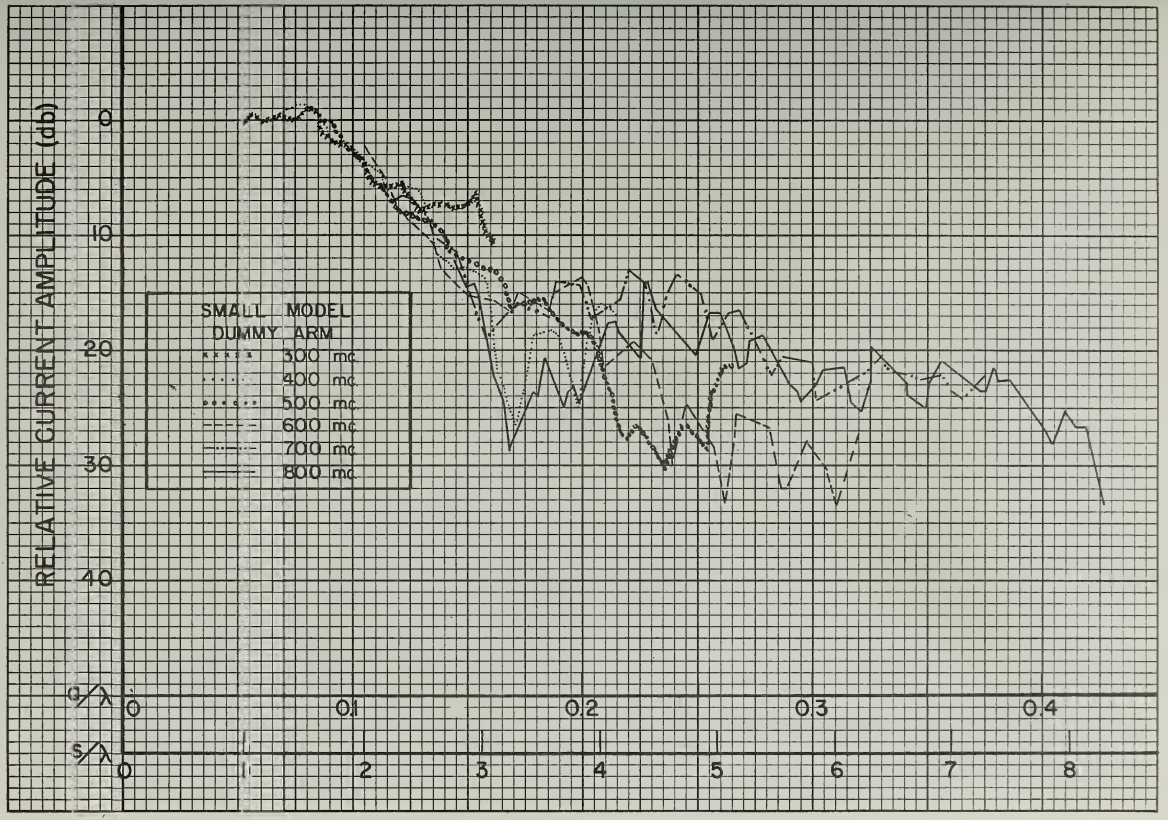

Figure 18. Composite curve of current amplitude along the arm as a function of frequency

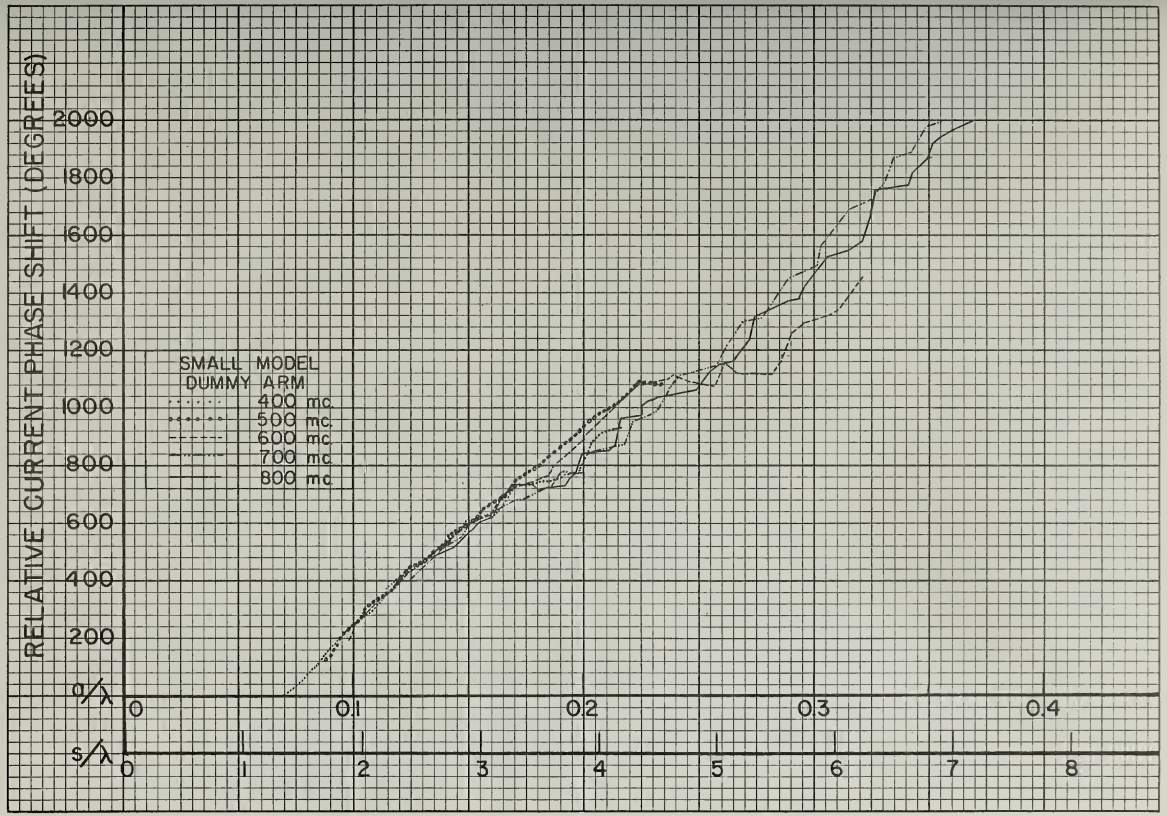

Figure 19. Composite curve of current phase shift along the arm as a function of frequency

In feeding the structure by the infinite balun method, it was evident that for operation at the lower frequencies the feed arm would have a different termination than the dummy arm. This gave a natural method to observe the base end effect on the current distribution at a low frequency. The relative magnitude was measured on both arms at 400 mc and is shown in Figure 20 The effects of the termination on the current distribution was rather obvious. It is interesting to note the rapidity with which the effect died out. This end effect is also demonstrated by comparing the data taken from both structures as was done in Figures 21, 22, and 23. In Figure 23, the end effect was not very evident, because both structures were, at 800 mc, rather large. The end effect at 800 mc was investigated by adding a $3/8\lambda$ extension to the dummy arm. It was felt that the small standing wave appearing in Figure 23 was not due to end effect as can be seen in Figure 24.

It was interesting to note, though, that the small standing wave had approximately the same period as the frequency of operation, i.e., half wave length nulls along the arm. Since this small standing wave was not due to a reflection, it was postulated that it was due to an interference between two different waves progressing in the same direction. This same phenomenon was observed by Marsh[11] when he measured the current distribution on a monofilar helical antenna. Marsh also demonstrated that a distribution similar to that shown in Figure 23 could be produced by a sum of four waves, two waves with different phase constants and their reflections. One of these waves had a phase constant equal to k, the phase constant of a free space wave, and the other had a phase constant approximately 1.4 k. The wave traveling at the speed of light was attenuated while the other was not. As was stated previously

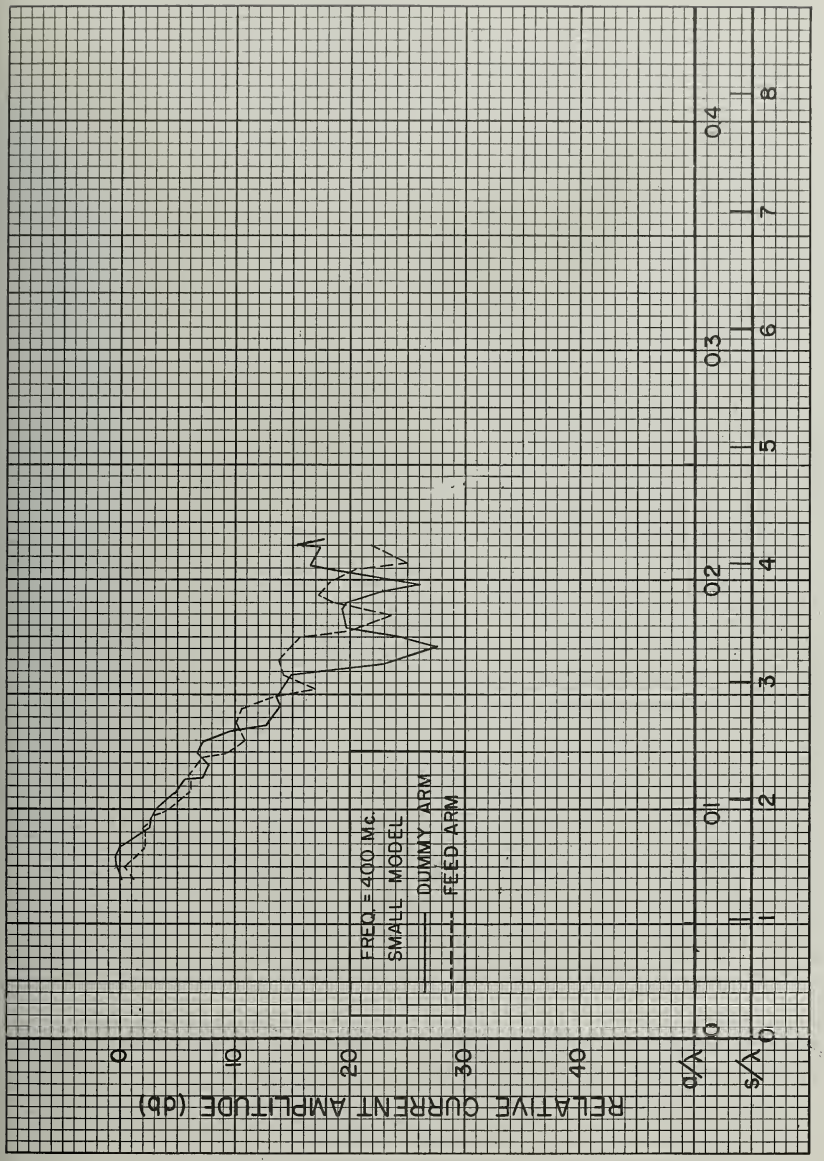

Figure 20. Comparison of current amplitude along both arms of the log-spiral at a low frequency

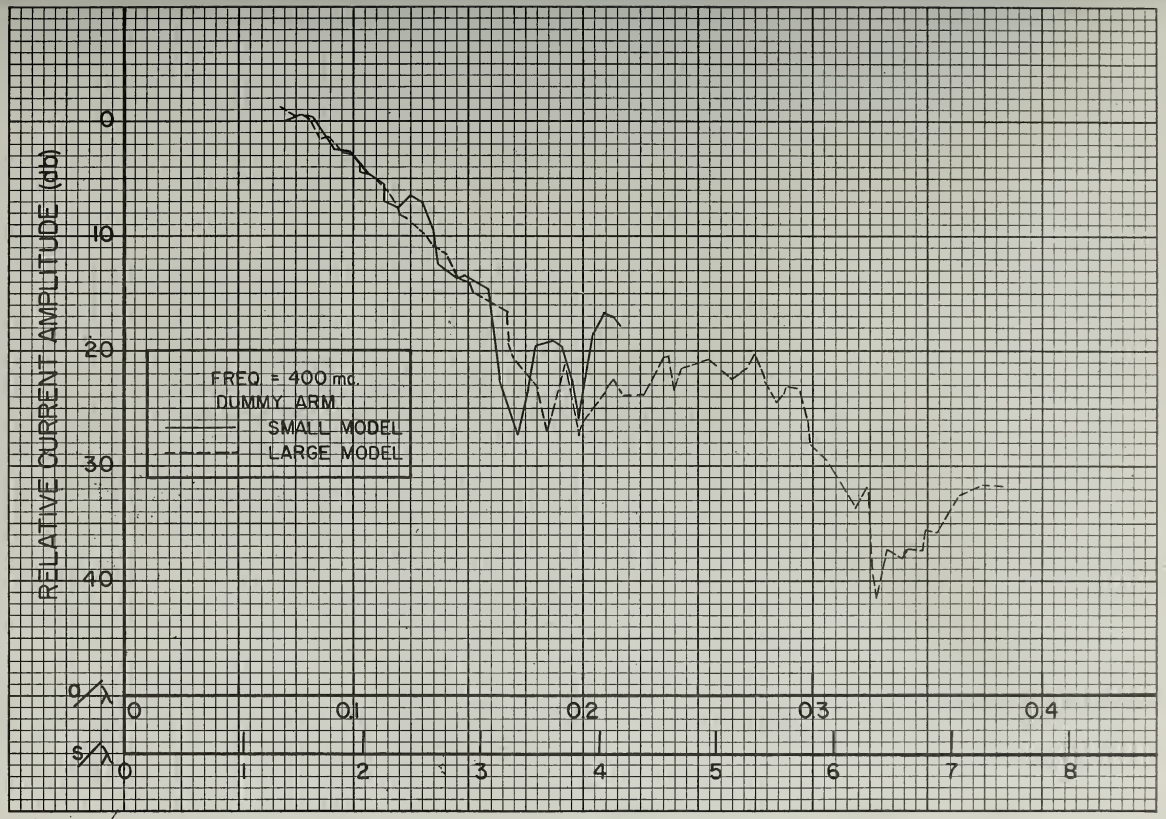

Figure 21. Comparison of the current amplitude along the dummy arms of both antennas at 400 mc

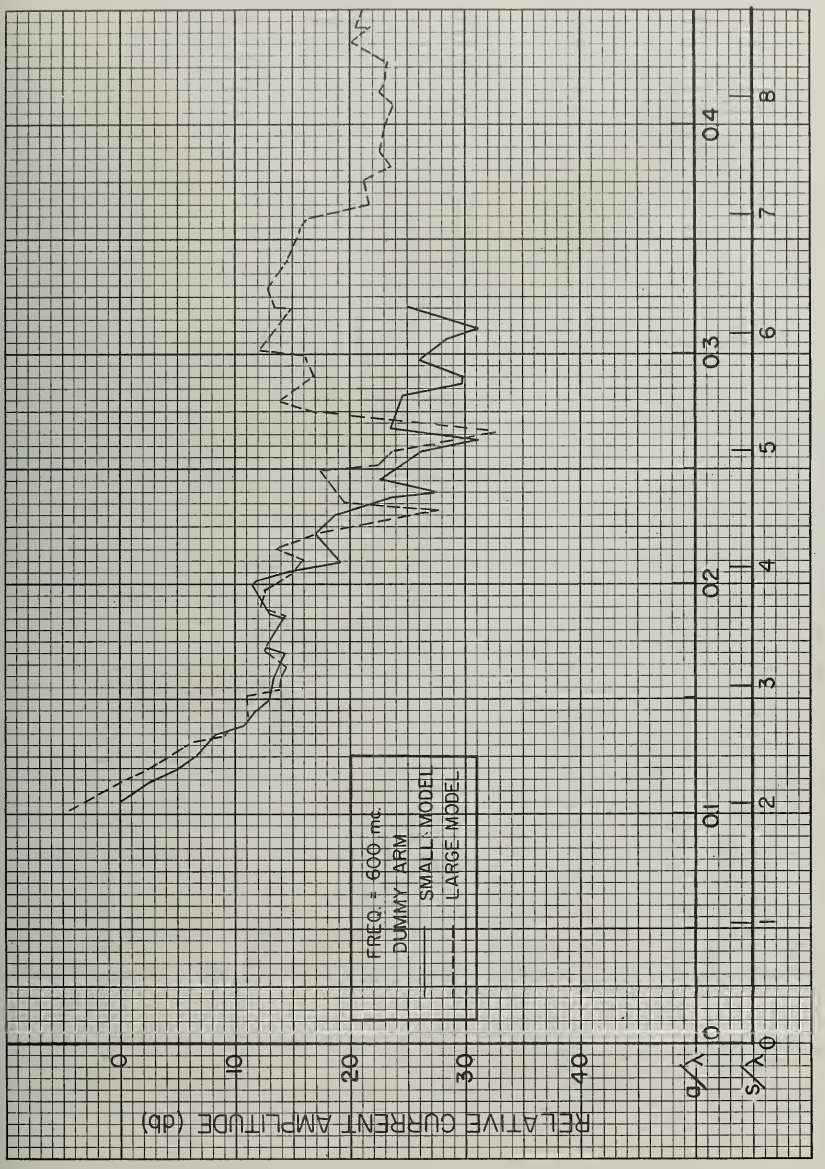

Figure 22. Comparison of the current amplitude along the dummy arms of both antennas at 600 mc

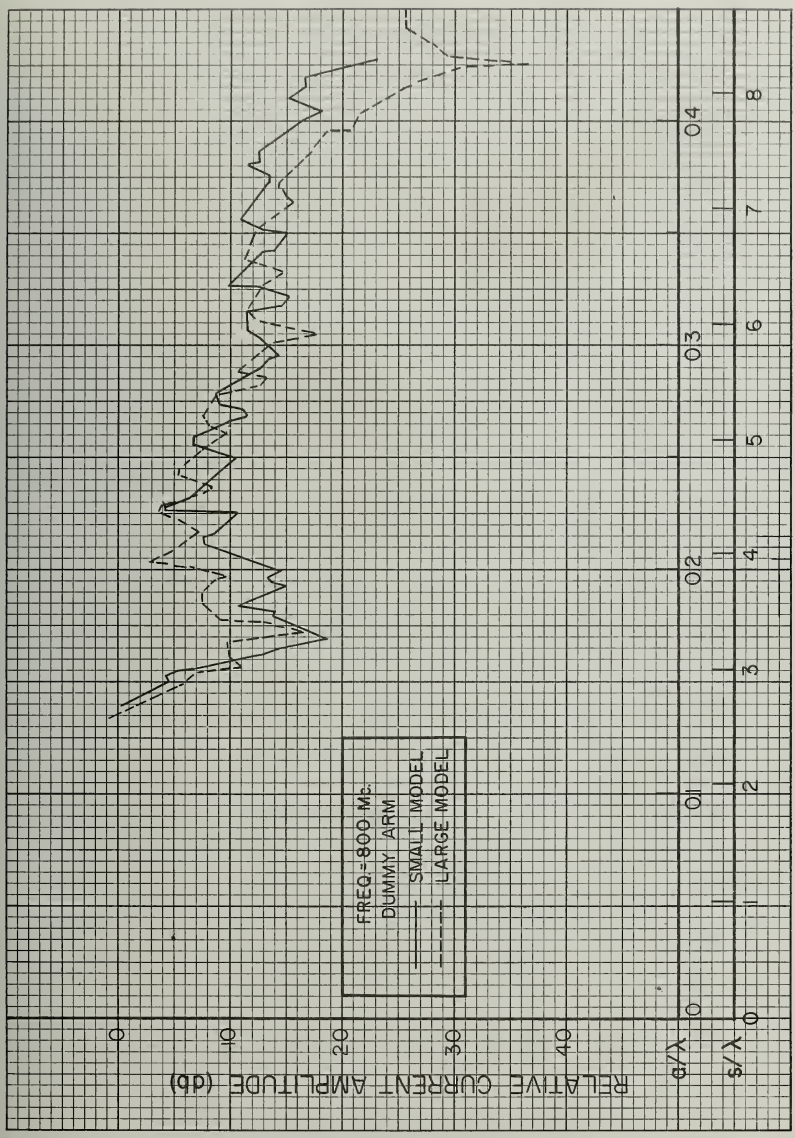

Figure 23. Comparison of the current amplitude along the dummy arms of both antennas at 800 mc

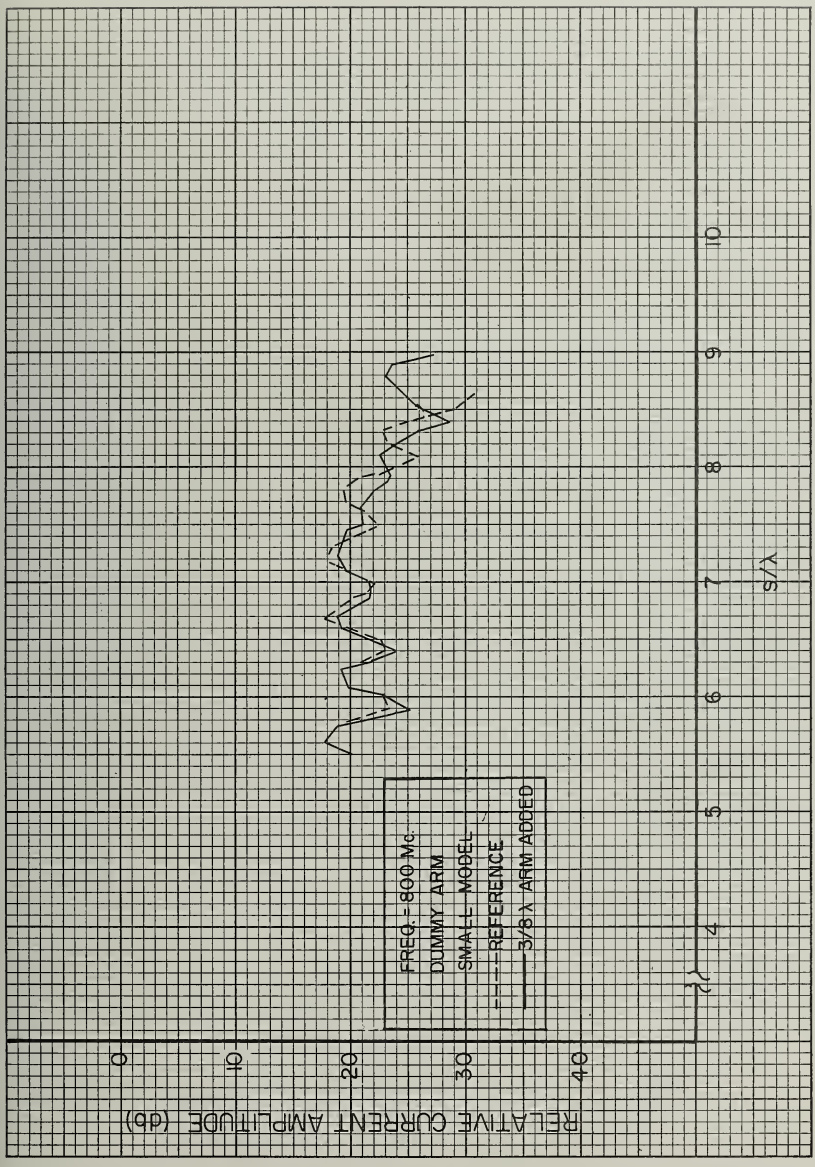

Figure 24. End effect at 800 mc on the small antenna

in Section 3, the fundamental wave had a phase constant approximately equal to k. The second wave could be explained as corresponding to a root following the $1 + ka/\cot \xi$ boundary line on the Brillouin diagram. By observing Figure 25, it is possible to see that at 800 mc the right hand root has an initial phase constant approximately 1.3 k. Therefore, it was quite reasonable to assume that there were two waves traveling in the same direction and that the second was being excited with sufficient amplitude such that its effects on the distribution were no longer negligible. By assuming the existence of this second wave, it is possible to explain the general nature of the amplitude curves[11]. It was felt that if only the fundamental wave, having a phase constant approximately equal to $2\pi/\lambda_o$, was present, that the amplitude curve would appear as in Figure 11. If the antenna was short enough in terms of wavelengths to allow reflections from the base, the fundamental wave and its reflection would yield a resultant as shown in Figure 13. If the two waves and small reflections from each were allowed, the distribution would appear as in Figures 14 through 17. By observing these five curves, it is possible to see the increasing effect of the second wave predicted by the k-β diagram.

In Figure 25 the amplitude measured at 400 mc has been plotted with the $ka/\cot \xi$ axis as its abscissa. This plot gives an opportunity to observe the variation in the current amplitude and the variation in β, both as a function of ka. Also on this chart, the location of the tip truncation has been plotted along the $k = \beta$ line as a function of frequency. At these frequencies, no values of β could exist which were below and to the left of these marks since these values indicate the location of the excitation.

Figure 26 is an average curve taken from the two composite curves shown in Figures 18 and 19. In Figure 26, the locations of the first, second, and third

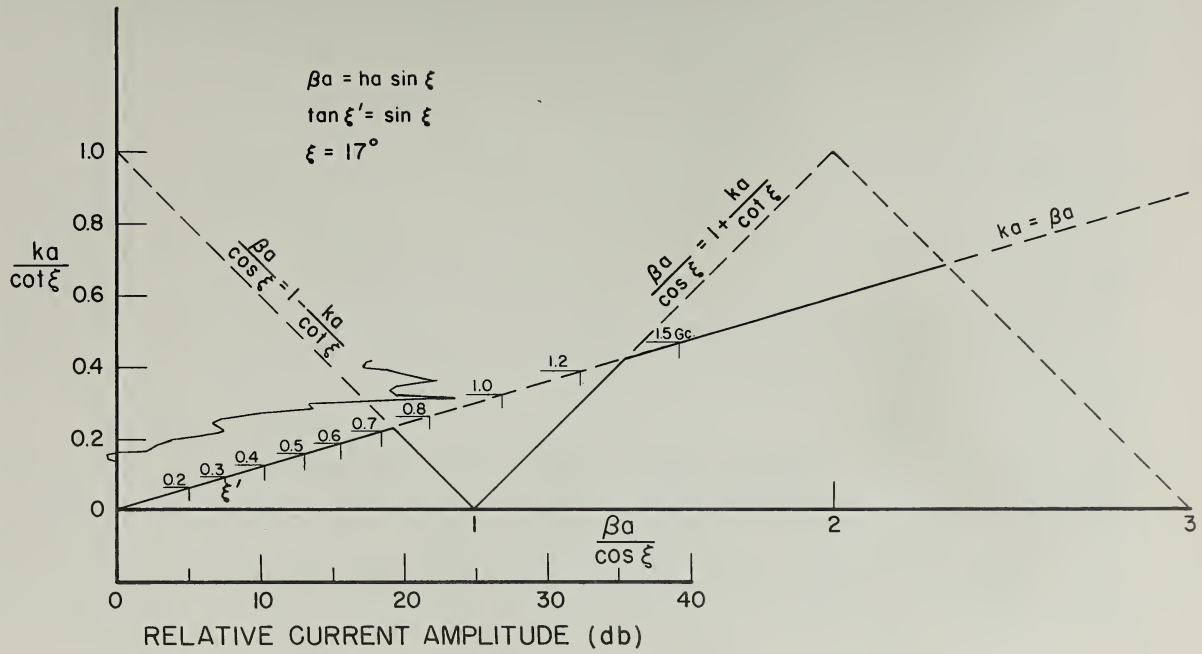

Figure 25. The current amplitude and location of the tip truncation superimposed on the k-β diagram

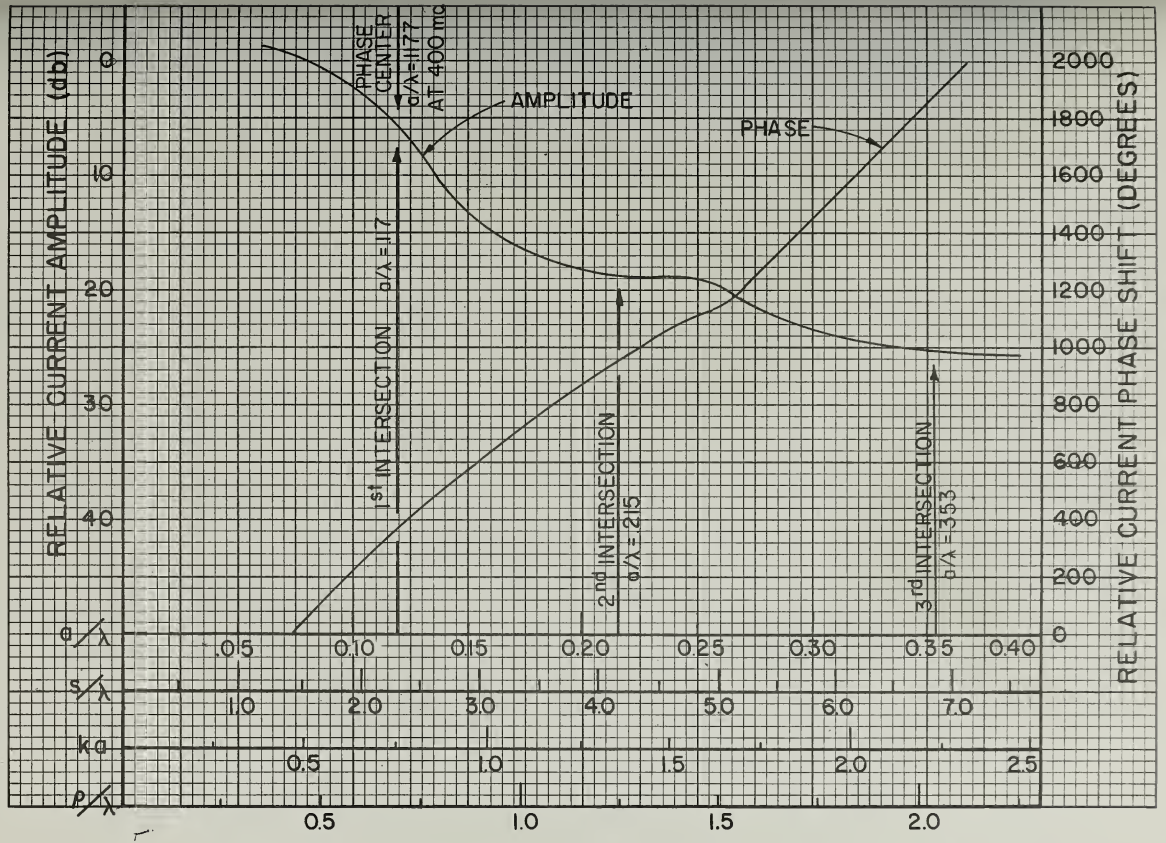

Figure 26. Average composite current distribution along the arm

intersections of the $k = \beta$ line and the boundary lines have been plotted Also the location of the phase center measured at 400 mc has been plotted It should be expected from observing Sensiper's work[6], that the structure should have begun to radiate before the first intersection was reached. This radiation, due to the phase constant β being complex, should have continued beyond the second intersection. Somewhere between the second and third intersections the phase constant should have again become real meaning that the wave would only propagate along the arm until the radius expanded to correspond to the third intersection where the phase constant again becomes complex.

From observing Figure 26 there seems to be a good correlation between the regions where β is complex and the regions where the amplitude decays rapidly, possibly indicating the physical regions which contribute appreciably to the radiation. This correlation is also confirmed by the fact that the phase center appears approximately in the middle of the region which has the highest rate of amplitude decay. Dyson has shown that the phase centers for wire arm conical equiangular spiral antennas consistently lie in this region and has developed a quasi-empirical formula for the position of the phase center[12,13].

In order to confirm that this initial region of decay was the only one contributing appreciably to radiation it would be necessary to calculate the far field radiation pattern using only the current distribution over this initial region and compare this pattern to one calculated using the complete data.

6.2 Electric Field Radiation Patterns and SWR Measurements

The electric field radiation patterns and the SWR referred to 50 ohms have

been measured on the small model. This data appears in Figures 27, 28, and 29. It is interesting to note the frequency range where the SWR is essentially constant. This appears to be from approximately 350 mc to 500 mc. This was the same region where only the fundamental wave and its reflection existed as was indicated by the current distribution curves. This same region can be observed in the patterns, (note the broadening of the beamwidth above 600 mc). The lower frequency patterns are modified by reflections from the surroundings but they do not indicate any appreciable sidelobes. At frequencies above 800 mc, it was obvious that the quasi dipole feed was radiating appreciably. According to the k-β diagram in Figure 25, at frequencies above 800 mc, the radiation should have been broadside, endfire, or a combination of these two. As can be seen, there was still a major lobe in the backfire direction. The most likely reason for this backward directed radiation was that the dipole feed section was radiating since it was greater than $3/8\lambda$ at these frequencies. The measured distance, from the apex of the cone to the phase center, in wavelengths has been shown in Figure 30. Superimposed upon this same chart is a plot of the distance, from the apex to the tip truncation, in terms of wavelengths. In order to have frequency independent operation, it is believed that the phase center should have remained essentially a constant distance, in wavelengths, from the apex. It can be seen though, that the tip truncation was influencing the location of the phase center as low as 600 mc[12]. Again this is approximately the same frequency at which the rest of the data began to deviate from that which one might associate with normal operation, i.e., one attenuated wave traveling approximately at the speed of light from the feed along the arm toward the base.

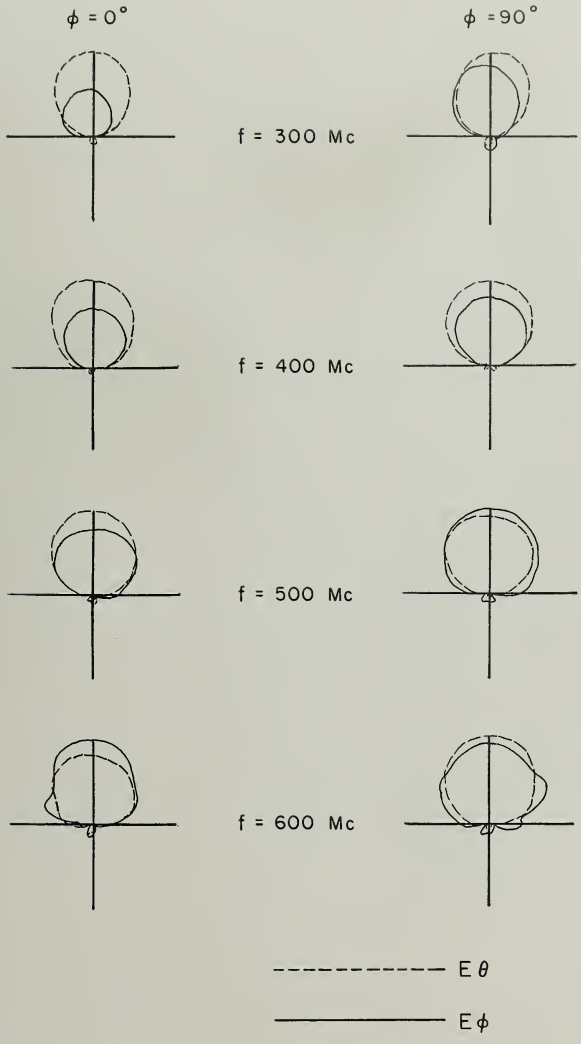

Figure 27. Electric field radiation patterns of the small antenna

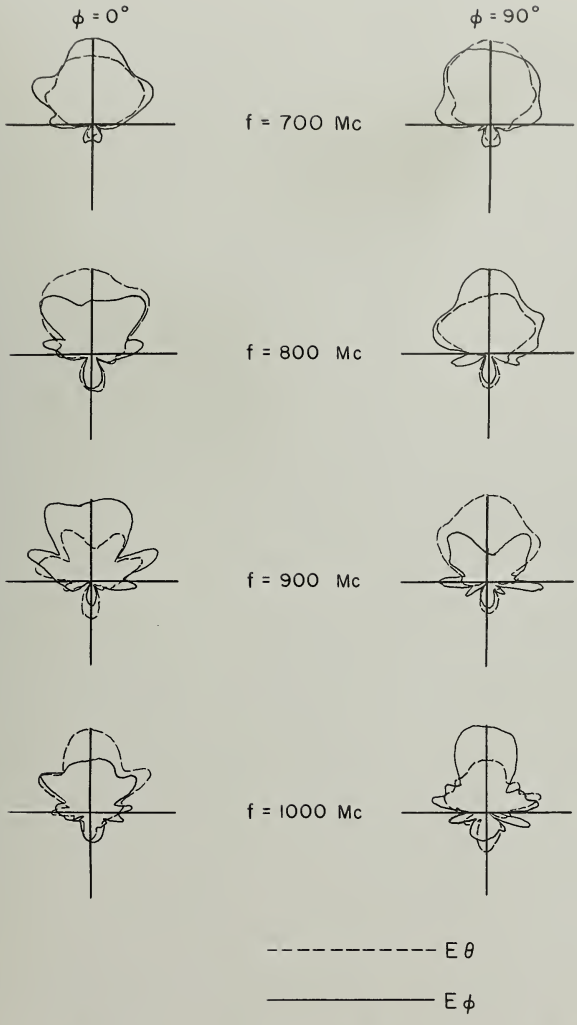

Figure 28. Electric field radiation patterns of the small antenna

Figure 29. Standing wave ratio referred to 50 Ω as a function of frequency

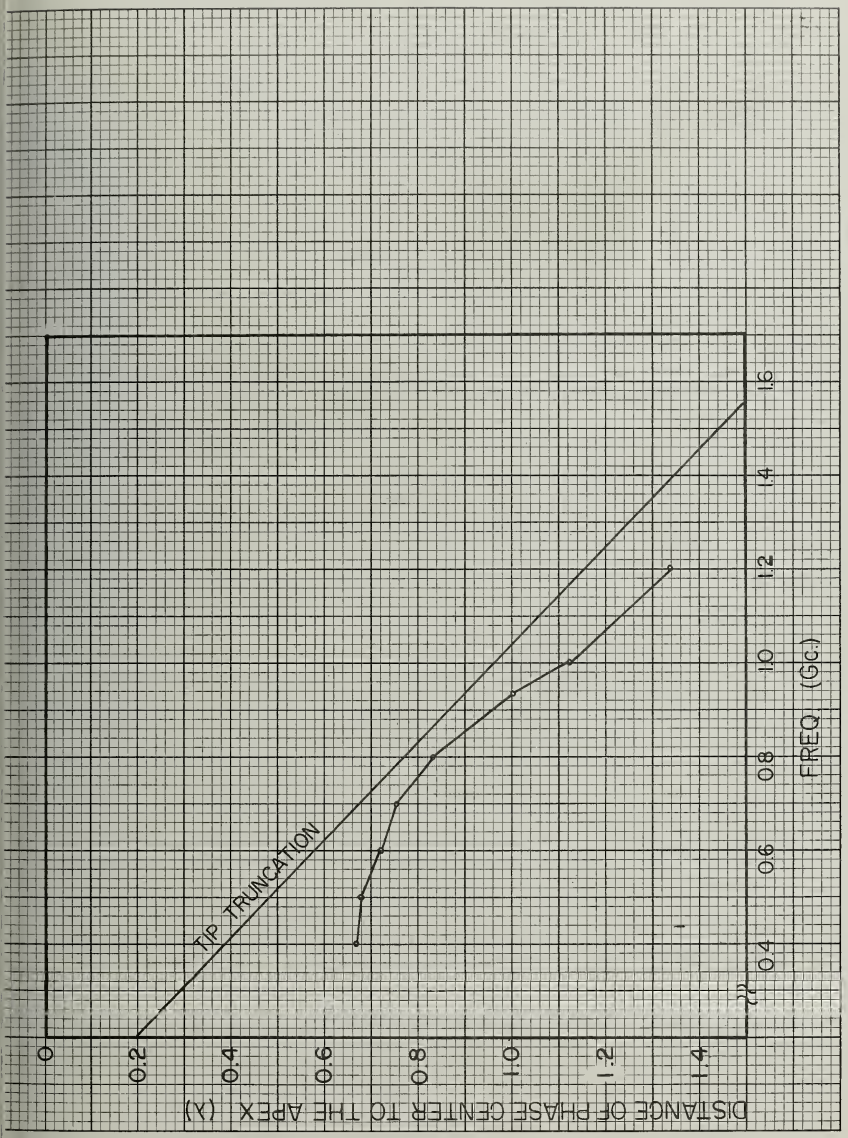

Figure 30. Relative distances of the phase center and tip truncation to the apex as a function of frequency

7. CONCLUSION

It was the purpose of these investigations to lead to a better understanding of the operation of the conical equiangular spiral antenna. The investigation was conducted by measuring the current distribution below, throughout, and above the normal frequency independent operating range. The phase center, far field patterns, and standing wave ratio were also measured. The results confirm the possibility of applying the general theory of backward wave radiation from periodic structures to the analysis of the radiation characteristics of the conical log-spiral antenna.

BIBLIOGRAPHY

1. Rumsey, V H., "Frequency Independent Antennas," I.R.E. National Convention Record, Pt. I, pp. 114-118, 1957. Also Technical Report No. 20, Contract AF33(616)-3220, Antenna Laboratory, University of Illinois, Urbana, Illinois, October, 1957.

2. Isbell, D. E., "Log Periodic Dipole," IRE Transactions, Vol. AP-8, No. 3, May 1960, pp. 260-267. Also Technical Report No. 39, Contract AF33(616)-6079, Antenna Laboratory, University of Illinois, Urbana, Illinois, June, 1959.

3. Carrel, R. L., "Analysis and Design of the Log-Periodic Dipole Antenna," Technical Report No. 52, Contract AF33(616)-6079, Antenna Laboratory, University of Illinois, Urbana, Illinois, October, 1961.

4. Dyson, J. D., "Recent Developments in Spiral Antennas," Proc. IRE National Aero. Elect. Conf., pp. 617-625, May, 1959.

5. Mayes, P. E., Deschamps, G. A., and Patton, W. T., "Backward-Wave Radiation from Periodic Structures and Applications to the Design of Frequency-Independent Antennas," Proc. IRE, Vol. 49, No. 5, pp. 962-963, May, 1961.

6. Brillouin, Leon, Wave Propagation in Periodic Structures, McGraw-Hill Book Company, Inc., 1946 or Dover Publications, Inc., 1953.

7. Sensiper, S., "Electromagnetic Wave Propagation on Helical Conductors," Technical Report No. 194, Res. Lab. of Elect., MIT, May 16, 1951.

8. Kogan, S. Kh., "The Propagation of Waves along an Endless Helix," C. R. Acad. Sci. U.R.S.S., 66, No. 5, p. 867, June 11, 1949. Referred to in Wireless Engineer, XXVIII, p. A.3, Item 30, January, 1951.

9. Renolds, D. K., "Surface-Current and Charge Measurements on Flat Metal Sheets," Technical Report No. 53, Contract N5ORI-76, Task Order No. 1, Nr-078-011, Cruft Laboratory, Harvard University, Cambridge, Massachusetts, August 1, 1948.

10. Dyson, J. D., "The Equiangular Spiral Antenna," IRE Transactions, Vol. AP-7, April, 1959, pp. 181-187. Also Technical Report No. 21, Contract AF33(616)-3220, Antenna Laboratory, University of Illinois, Urbana, Illinois, September, 1957.

11. Marsh, J. A., "Current Distributions on Helical Antennas," Proc. IRE, Vol. 39, pp. 668-675, Project Report No. 339-10 from the Ohio State University Research Foundation, a portion of a S.S.C. Thesis, Ohio State University, 1949.

12. Dyson, J. D., "On the Radiation from the Conical Log-Spiral Antenna," Internal. Technical Memorandum 62-1, Antenna Laboratory, Univ. of Ill., January 22, 1962 (Unpublished).

BIBLIOGRAPHY (Continued)

13. Dyson, J. D., "The Coupling and Mutual Impedance between Conical Log-Spiral Antennas in Simple Arrays," IRE International Convention Record Part I, March, 1962.

AF33(657)-8460

DISTRIBUTION LIST

One copy each unless otherwise indicated

Armed Services Technical Information Agency
Attn: TIP-DR
Arlington Hall Station
Arlington 12, Virginia (10 copies)

Aeronuatical Systems Division
Attn: (ASRNRE-4)
Wright-Patterson Air Force Base
Ohio (3 copies)

Aeronautical Systems Division
Attn: ASDSED, Mr. Mulligan
Wright-Patterson Air Force Base
Ohio

Aeronautical Systems Division
Attn: AFCIN-4B1A
Wright-Patterson Air Force Base
Ohio

Air Force Cambridge Research Laboratory
Attn: CRRD
Laurence G. Hanscom Field
Bedford, Massachusetts

Commander
Air Force Missile Test Center
Patrick Air Force Base
Florida

Commander
Air Force Missile Development Center
Attn: Technical Library
Holloman Air Force Base
New Mexico

Air Force Ballistic Missile Division
Attn: Technical Library, Air Force Unit Post Office
Los Angeles, California

Director
Ballistics Research Laboratory
Attn: Ballistics Measurement Lab.
Aberdeen Proving Ground, Maryland

National Aeronautics & Space Adm.
Attn: Librarian
Langley Field, Virginia

Rome Air Development Center
Attn: RCLTM
Griffiss Air Force Base
New York

Research & Development Command
Hq. USAF (ARDRD-RE)
Washington 25, D. C.

Office of Chief Signal Officer
Engineering & Technical Division
Attn: SIGNET-5
Washington 25, D. C.

Commander
U. S. Army White Sands Signal Agency
Attn: SIGWS-FC-02
White Sands, New Mexico

Director
Surveillance Department
Evans Area
Attn: Technical Document Center
Belman, New Jersey

Commander
U. S. Naval Air Test Center
Attn: WST-54, Antenna Section
Patuxent River, Maryland

Material Laboratory, Code 932
New York Naval Shipyard
Brooklyn 1, New York

Commanding Officer
Diamond Ordnance Fuse Laboratories
Attn: 240
Washington 25, D. C.

Director
U. S. Navy Electronics Laboratory
Attn: Library
San Diego 52, California

Adams-Russell Company
200 Sixth Street
Attn: Library (Antenna Section)
Cambridge, Massachusetts

Aero Geo Astro
Attn: Security Officer
1200 Duke Street
Alexandria, Virginia

NASA Goddard Space Flight Center
Attn: Antenna Section, Code 523
Greenbelt, Maryland

Airborne Instruments Labs., Inc.
Attn: Librarian (Antenna Section)
Walt Whitman Road
Melville, L. I., New York

American Electronic Labs
Box 552 (Antenna Section)
Lansdale, Pennsylvania

Andrew Alfred Consulting Engineers
Attn: Librarian (Antenna Section)
299 Atlantic Ave.
Boston 10, Massachusetts

Ampheol-Borg Electronic Corporation
Attn: Librarian (Antenna Section)
2801 S. 25th Avenue
Broadview, Illinois

Bell Aircraft Corporation
Attn: Technical Library
(Antenna Section)
Buffalo 5, New York

Bendix Radio Division of
Bendix Aviation Corporation
Attn: Technical Library
(For Dept. 462-4)
Baltimore 4, Maryland

Boeing Airplane Company
Aero Space Division
Attn: Technical Library
M/F Antenna & Radomes Unit
Seattle, Washington

Boeing Airplane Company
Attn: Technical Library
M/F Antenna Systems Staff Unit
Wichita, Kansas

Chance Vought Aircraft Inc.
THRU: BU AER Representative
Attn: Technical Library
M/F Antenna Section
P. O. Box 5907
Ballas 22, Texas

Collins Radio Company
Attn: Technical Library (Antenna
Section)
Dallas, Texas

Convair
Ft. Worth Division
Attn: Technical Library (Antenna
Section)
Grants Lane
Fort Worth, Texas

Convair
Attn: Technical Library (Antenna
Section)
P. O. Box 1050
San Diego 12, California

Dalmo Victor Company
Attn: Technical Library (Antenna
Section)
1515 Industrial Way
Belmont, California

Dorne & Margolin, Inc.
Attn: Technical Library (Antenna
Section)
30 Sylvester Street
Westbury, L. I., New York

Dynatronics Inc.
Attn: Technical Library (Antenna
Section)
Orlando, Florida

Electronic Communications, Inc.
Research Division
Attn: Technical Library
1830 York Road
Timonium, Maryland

Fairchild Engine & Airplane Corporation
Fairchild Aircraft & Missiles Division
Attn: Technical Library (Antenna Section)
Hagerstown 10, Maryland

Georgia Institute of Technology
Engineering Experiment Station
Attn: Technical Library
M/F Electronics Division
Atlanta 13, Georgia

General Electric Company
Electronics Laboratory
Attn: Technical Library
Electronics Park
Syracuse, New York

General Electronic Labs., Inc.
Attn: Technical Library (Antenna Section)
18 Ames Street
Cambridge 42, Massachusetts

General Precision Lab., Division of General Precision Inc.
Attn: Technical Library (Antenna Section)
63 Bedford Road
Pleasantville, New York

Goodyear Aircraft Corporation
Attn: Technical Library
M/F Dept. 474
1210 Massilon Road
Akron 15, Ohio

Granger Associates
Attn: Technical Library (Antenna Section)
974 Commercial Street
Palo Alto, California

Grumman Aircraft Engineering Corp.
Attn: Technical Library
M/F Avionics Engineering
Bethpage, New York

The Hallicrafters Company
Attn: Technical Library (Antenna Section)
4401 W. Fifth Avenue
Chicago 24, Illinois

Hoffman Laboratories Inc.
Attn: Technical Library (Antenna Section)
Los Angeles 7, California

John Hopkins University
Applied Physics Laboratory
8621 Georgia Avenue
Silver Springs, Maryland

Hughes Aircraft Corporation
Attn: Technical Library (Antenna Section)
Florence & Teal Street
Culver City, California

ITT Laboratories
Attn: Technical Library (Antenna Section)
500 Washington Avenue
Nutley 10, New Jersey

U. S. Naval Ordnance Lab.
Attn: Technical Library
Corona, California

Lincoln Laboratories
Massachusetts Institute of Technology
Attn: Document Room
P. O. Box 73
Lexington 73, Massachusetts

Litton Industries
Attn: Technical Library (Antenna Section)
4900 Calvert Road
College Park, Maryland

Lockheed Missile & Space Division
Attn: Technical Library (M/F Dept-58-40, Plant 1, Bldg. 130)
Sunnyvale, California

The Martin Company
Attn: Technical Library (Antenna Section)
P. O. Box 179
Denver 1, Colorado

The Martin Company
Attn: Technical Library (Antenna Section)
Baltimore 3, Maryland

The Martin Company
Attn: Technical Library (M/F Microwave Laboratory)
Box 5837
Orlando, Florida

W. L. Maxson Corporation
Attn: Technical Library (Antenna Section)
460 West 34th Street
New York 1, New York

McDonnell Aircraft Corporation
Attn: Technical Library (Antenna Section)
Box 516
St. Louis 66, Missouri

Melpar, Inc.
Attn: Technical Library (Antenna Section)
3000 Arlington Blvd.
Falls Church, Virginia

University of Michigan
Radiation Laboratory
Willow Run
201 Catherine Street
Ann Arbor, Michigan

Mitre Corporation
Attn: Technical Library (M/F Electtronic Warfare Dept. D-21)
Middlesex Turnpike
Bedford, Massachusetts

North American Aviation Inc.
Attn: Technical Library (M/F Engineering Dept.)
4300 E. Fifth Avenue
Columbus 16, Ohio

North American Aviation Inc.
Attn: Technical Library (M/F Dept. 56)
International Airport
Los Angeles, California

Northrop Corporation
NORAIR Division
1001 East Broadway
Attn: Technical Information (3924-3)
Hawthorne, California

Ohio State University Research Foundation
Attn: Technical Library (M/F Antenna Laboratory)
1314 Kinnear Road
Columbus 12, Ohio

Philco Corporation
Government & Industrial Division
Attn: Technical Library (M/F Antenna Section)
4700 Wissachickon Avenue
Philadelphia 44, Pennsylvania

Westinghouse Electric Corporation
Air Arms Division
Attn: Librarian (Antenna Lab)
P. O. Box 746
Baltimore 3, Maryland

Wheeler Laboratories
Attn: Librarian (Antenna Lab)
Box 561
Smithtown, New York

Electrical Engineering Research Laboratory
University of Texas
Box 8026, Univ. Station
Austin, Texas

University of Michigan Research Institute
Electronic Defense Group
Attn: Dr. J. A. M. Lyons
Ann Arbor, Michigan

Radio Corporation of America
RCA Laboratories Division
Attn: Technical Library
(M/F Antenna Section)
Princeton, New Jersey

Radiation, Inc.
Attn: Technical Library (M/F)
Antenna Section
Drawer 37
Melbourne, Florida

Radioplane Company
Attn: Librarian (M/F Aerospace Lab)
8000 Woodly Avenue
Van Nuys, California

Ramo-Wooldridge Corporation
Attn: Librarian (Antenna Lab)
Conoga Park, California

Rand Corporation
Attn: Librarian (Antenna Lab)
1700 Main Street
Santa Monica, California

Rantec Corporation
Attn: Librarian (Antenna Lab)
23999 Ventura Blvd.
Calabasas, California

Raytheon Electronics Corporation
Attn: Librarian (Antenna Lab)
1089 Washington Street
Newton, Massachusetts

Republic Aviation Corporation
Applied Research & Development
Division
Attn: Librarian (Antenna Lab)
Farmingdale, New York

Sanders Associates
Attn: Librarian (Antenna Lab)
95 Canal Street
Nashua, New Hampshire

Southwest Research Institute
Attn: Librarian (Antenna Lab)
8500 Culebra Road
San Antonio, Texas

H. R. B. Singer Corporation
Attn: Librarian (Antenna Lab)
State College, Pennsylvania

Sperry Microwave Electronics Company
Attn: Librarian (Antenna Lab)
P. O. Box 1828
Clearwater, Florida

Sperry Gyroscope Company
Attn: Librarian (Antenna Lab)
Great Neck, L. I., New York

Stanford Electronic Laboratory
Attn: Librarian (Antenna Lab)
Stanford, California

Stanford Research Institute
Attn: Librarian (Antenna Lab)
Menlo Park, California

Sylvania Electronic System
Attn: Librarian (M/F Antenna &
Microwave Lab)
100 First Street
Waltham 54, Massachusetts

Sylvania Electronic System
Attn: Librarian (Antenna Lab)
P. O. Box 188
Mountain View, California

Technical Research Group
Attn: Librarian (Antenna Section)
2 Aerial Way
Syosset, New York

Ling Temco Aircraft Corporation
Temco Aircraft Division
Attn: Librarian (Antenna Lab)
Garland, Texas

Texas Instruments, Inc.
Attn: Librarian (Antenna Lab)
6000 Lemmon Ave.
Dallas 9, Texas

A. S. Thomas, Inc.
Attn: Librarian (Antenna Lab)
355 Providence Highway
Westwood, Massachusetts

New Mexico State University
Head Antenna Department
Physical Science Laboratory
University Park, New Mexico

Bell Telephone Laboratories, Inc.
Whippany Laboratory
Whippany, New Jersey
Attn: Technical Reports Librarian
Room 2A-165

Robert C. Hansen
Aerospace Corporation
Box 95085
Los Angeles 45, California

Dr. Richard C. Becker
10829 Berkshire
Westchester, Illinois

Dr. Harry Letaw, Jr.
Raytheon Company
Surface Radar and Navigation
Operations
State Road West
Wayland, Massachusetts

Dr. Frank Fu Fang
IBM Research Laboratory
Poughkeepsie, New York

Mr. Dwight Isbell
1422 11th West
Seattle 99, Washington

Dr. Robert L. Carrel
Collins Radio Corporation
Antenna Section
Dallas, Texas

Dr. A. K. Chatterjee
Vice Principal & Head of the Department
of Research
Birla Institute of Technology
P. O. Mesra
District-Ranchi (Bihar) India

Aeronautical Systems Division
Attn: ASAD - Library
Wright-Patterson Air Force Base
Ohio

National Bureau of Standards
Department of Commerce
Attn: Dr. A. G. McNish
Washington 25, D. C.

ANTENNA LABORATORY
TECHNICAL REPORTS AND MEMORANDA ISSUED

ontract AF33(616)-310

Synthesis of Aperture Antennas," Technical Report No. 1, C.T.A. Johnk, ctober, 1954.*

A Synthesis Method for Broad-band Antenna Impedance Matching Networks," echnical Report No. 2, Nicholas Yaru, 1 February 1955.* AD 61049.

The Assymmetrically Excited Spherical Antenna," Technical Report No. 3, obert C. Hansen, 30 April 1955.*

Analysis of an Airborne Homing System," Technical Report No. 4, Paul E. ayes, 1 June 1955 (CONFIDENTIAL).

Coupling of Antenna Elements to a Circular Surface Waveguide," Technical eport No. 5, H. E. King and R. H. DuHamel, 30 June 1955.*

Axially Excited Surface Wave Antennas," Technical Report No. 7, D. E. Royal,) October 1955.*

Homing Antennas for the F-86F Aircraft (450-2500 mc)," Technical Report No. 8, . E. Mayes, R. F. Hyneman, and R. C. Becker, 20 February 1957, (CONFIDENTIAL).

Ground Screen Pattern Range," Technical Memorandum No. 1, Roger R. Trapp,) July 1955.*

ontract AF33(616)-3220

Effective Permeability of Spheroidal Shells," Technical Report No. 9, E. J. cott and R. H. DuHamel, 16 April 1956.

An Analytical Study of Spaced Loop ADF Antenna Systems," Technical Report o. 10, D. G. Berry and J. B. Kreer, 10 May 1956. AD 98615

A Technique for Controlling the Radiation from Dielectric Rod Waveguides," echnical Report No. 11, J. W. Duncan and R. H. DuHamel, 15 July 1956.*

Directional Characteristics of a U-Shaped Slot Antenna," Technical Report o. 12, Richard C. Becker, 30 September 1956.**

Impedance of Ferrite Loop Antennas," Technical Report No. 13, V. H. Rumsey nd W. L. Weeks, 15 October 1956. AD 119780

Closely Spaced Transverse Slots in Rectangular Waveguide," Technical Report o. 14, Richard F. Hyneman, 20 December 1956.

"Distributed Coupling to Surface Wave Antennas," Technical Report No. 15, Ralph Richard Hodges, Jr., 5 January 1957.

"The Characteristic Impedance of the Fin Antenna of Infinite Length," Technical Report No. 16, Robert L. Carrel, 15 January 1957.*

"On the Estimation of Ferrite Loop Antenna Impedance," Technical Report No. 17, Walter L. Weeks, 10 April 1957.* AD 143989

"A Note Concerning a Mechanical Scanning System for a Flush Mounted Line Source Antenna," Technical Report No. 18, Walter L. Weeks, 20 April 1957.

"Broadband Logarithmically Periodic Antenna Structures," Technical Report No. 19, R. H. DuHamel and D. E. Isbell, 1 May 1957. AD 140734

"Frequency Independent Antennas," Technical Report No. 20, V. H. Rumsey, 25 October 1957.

"The Equiangular Spiral Antenna," Technical Report No. 21, J. D. Dyson, 15 September 1957. AD 145019

"Experimental Investigation of the Conical Spiral Antenna," Technical Report No. 22, R. L. Carrel, 25 May 1957.** AD 144021

"Coupling between a Parallel Plate Waveguide and a Surface Waveguide," Technical Report No. 23, E. J. Scott, 10 August 1957.

"Launching Efficiency of Wires and Slots for a Dielectric Rod Waveguide," Technical Report No. 24, J. W. Duncan and R. H. DuHamel, August 1957.

"The Characteristic Impedance of an Infinite Biconical Antenna of Arbitrary Cross Section," Technical Report No. 25, Robert L. Carrel, August 1957.

"Cavity-Backed Slot Antennas," Technical Report No. 26, R. J. Tector, 30 October 1957.

"Coupled Waveguide Excitation of Traveling Wave Slot Antennas," Technical Report No. 27, W. L. Weeks, 1 December 1957.

"Phase Velocities in Rectangular Waveguide Partially Filled with Dielectric," Technical Report No. 28, W. L. Weeks, 20 December 1957.

"Measuring the Capacitance per Unit Length of Biconical Structures of Arbitrary Cross Section," Technical Report No. 29, J. D. Dyson, 10 January 1958.

"Non-Planar Logarithmically Periodic Antenna Structure," Technical Report No. 30, J. E. Isbell, 20 February 1958. AD 156203

"Electromagnetic Fields in Rectangular Slots," Technical Report No. 31, N. J. Kuhn and P. E. Mast, 10 March 1958.

"The Efficiency of Excitation of a Surface Wave on a Dielectric Cylinder," Technical Report No. 32, J. W. Duncan, 25 May 1958.

"A Unidirectional Equiangular Spiral Antenna," Technical Report No. 33, J. D. Dyson, 10 July 1958. AD 201138

"Dielectric Coated Spheriodal Radiators," Technical Report No. 34, W. L. Weeks, 12 September 1958. AD 204547

"A Theoretical Study of the Equiangular Spiral Antenna," Technical Report No. 35, P. E. Mast, 12 September 1958. AD 204548

Contract AF33(616)-6079

"Use of Coupled Waveguides in a Traveling Wave Scanning Antenna," Technical Report No. 36, R. H. MacPhie, 30 April 1959. AD 215558

"On the Solution of a Class of Wiener-Hopf Integral Equations in Finite and Infinite Ranges," Technical Report No. 37, Raj Mittra, 15 May 1959.

"Prolate Spheroidal Wave Functions for Electromagnetic Theory," Technical Report No. 38, W. L. Weeks, 5 June 1959.

"Log Periodic Dipole Arrays," Technical Report No. 39, D. E. Isbell, 1 June 1959. AD 220651

"A Study of the Coma-Corrected Zoned Mirror by Diffraction Theory," Technical Report No. 40, S. Dasgupta and Y. T. Lo, 17 July 1959.

"The Radiation Pattern of a Dipole on a Finite Dielectric Sheet," Technical Report No. 41, K. G. Balmain, 1 August 1959.

"The Finite Range Wiener-Hopf Integral Equation and a Boundary Value Problem in a Waveguide," Technical Report No. 42, Raj Mittra, 1 October 1959.

"Impedance Properties of Complementary Multiterminal Planar Structures," Technical Report No. 43, G. A. Deschamps, 11 November 1959.

"On the Synthesis of Strip Sources," Technical Report No. 44, Raj Mittra, 1 December 1959.

"Numerical Analysis of the Eigenvalue Problem of Waves in Cylindrical Waveguides," Technical Report No. 45, C. H. Tang and Y. T. Lo, 11 March 1960.

"New Circularly Polarized Frequency Independent Antennas with Conical Beam or Omnidirectional Patterns," Technical Report No. 46, J. D. Dyson and P. E. Mayes, 10 June 1960. AD 241321

"Logarithmically Periodic Resonant-V Arrays," Technical Report No. 47, P. E. Mayes, and R. L. Carrel, 15 July 1960. AD 246302

"A Study of Chromatic Aberration of a Coma-Corrected Zoned Mirror," Technical Report No. 48, Y. T. Lo, June 1960

"Evaluation of Cross-Correlation Methods in the Utilization of Antenna Systems," Technical Report No. 49, R. H. MacPhie, 25 January 1961

"Synthesis of Antenna Product Patterns Obtained from a Single Array," Technical Report No. 50, R. H. MacPhie, 25 January 1961.

"On the Solution of a Class of Dual Integral Equations," Technical Report No. 51, R. Mittra, 1 October 1961. AD 264557

"Analysis and Design of the Log-Periodic Dipole Antenna," Technical Report No. 52, Robert L. Carrel, 1 October 1961.* AD 264558

"A Study of the Non-Uniform Convergence of the Inverse of a Doubly-Infinite Matrix Associated with a Boundary Value Problem in a Waveguide," Technical Report No. 53, R. Mittra, 1 October 1961. AD 264556

Copies available for a three-week loan period.

* Copies no longer available.